Fig 5

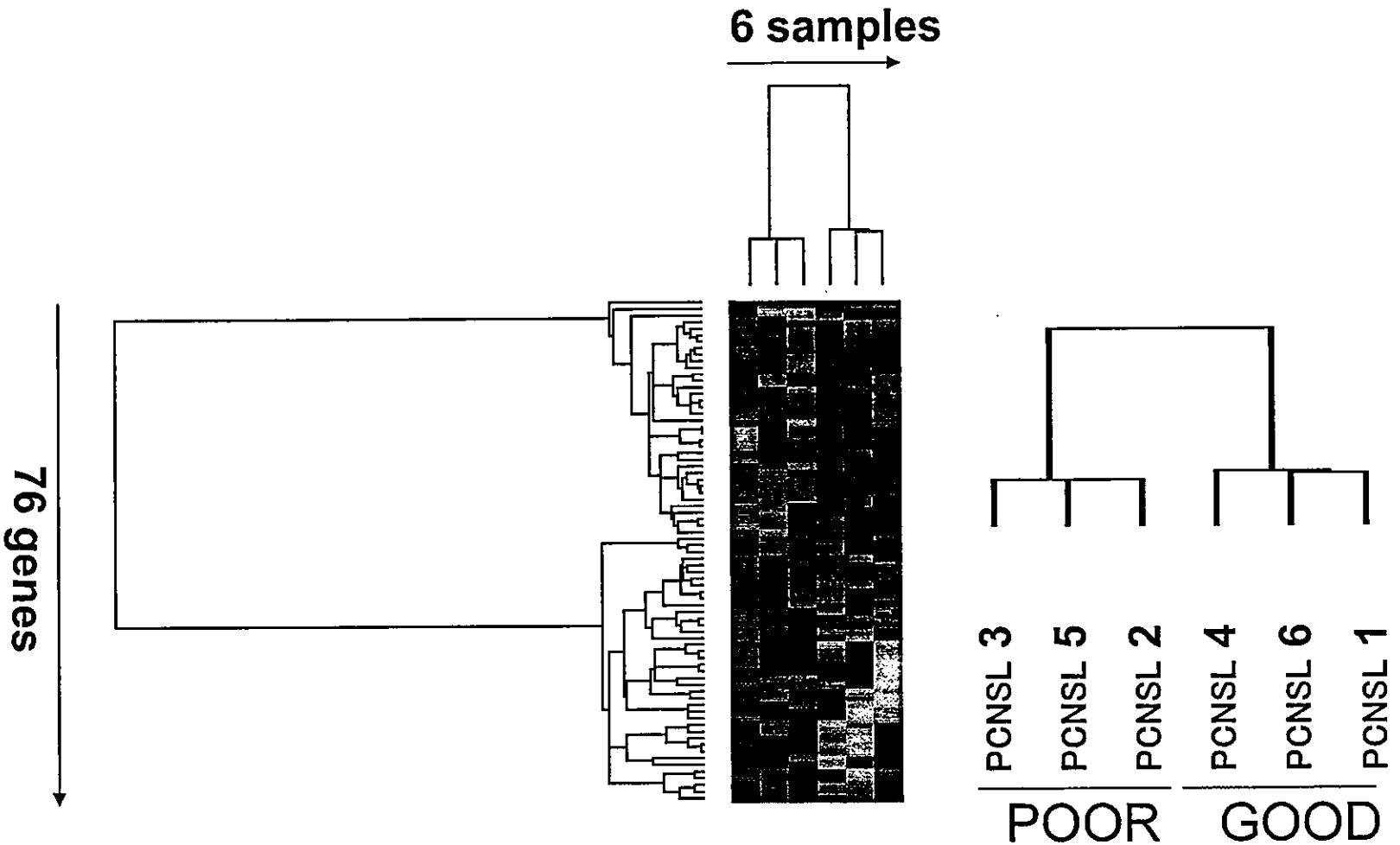
6 samples
76 genes
PCNSL 3
PCNSL 5
PCNSL 2
PCNSL 4
PCNSL 6
PCNSL 1
POOR
GOOD

Fig 6

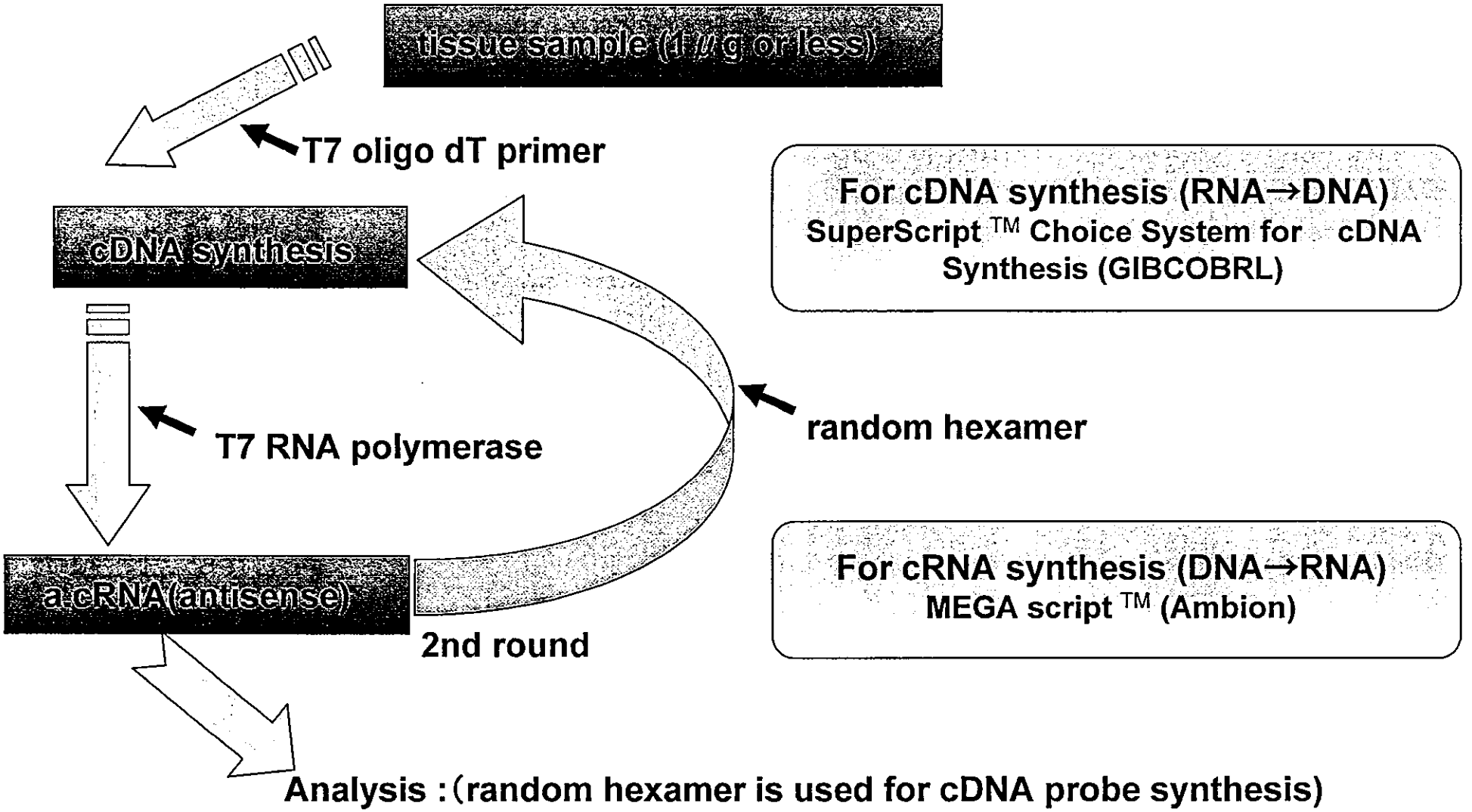
178
tissue sample (1 μg or less)
T7 oligo dT primer
cDNA synthesis
For cDNA synthesis (RNA→DNA)
SuperScript ™ Choice System for cDNA Synthesis (GIBCOBRL)
T7 RNA polymerase
random hexamer
a cRNA(antisense)
For cRNA synthesis (DNA→RNA)
MEGA script ™ (Ambion)
2nd round
Analysis : (random hexamer is used for cDNA probe synthesis)

Fig 7

# Is differential expression conserved even after amplification?



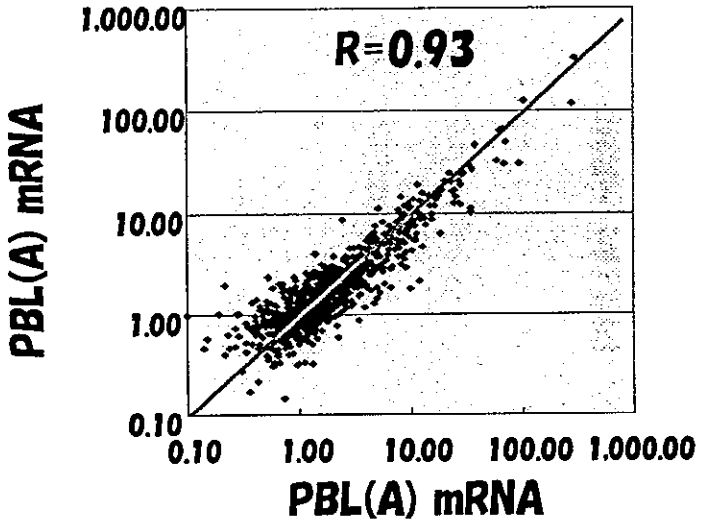


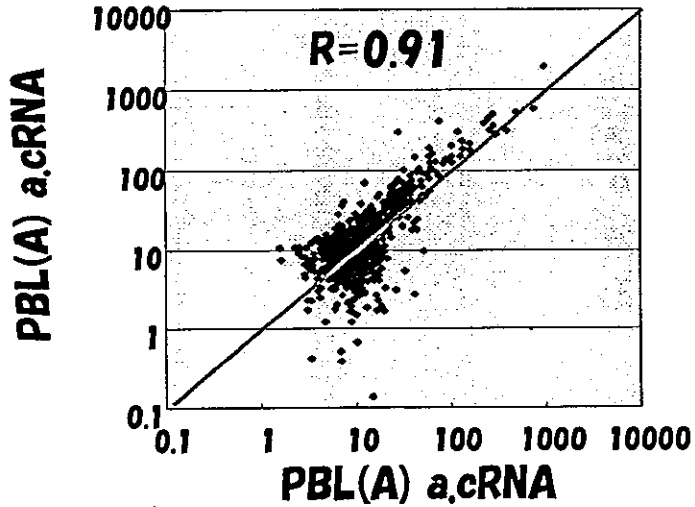


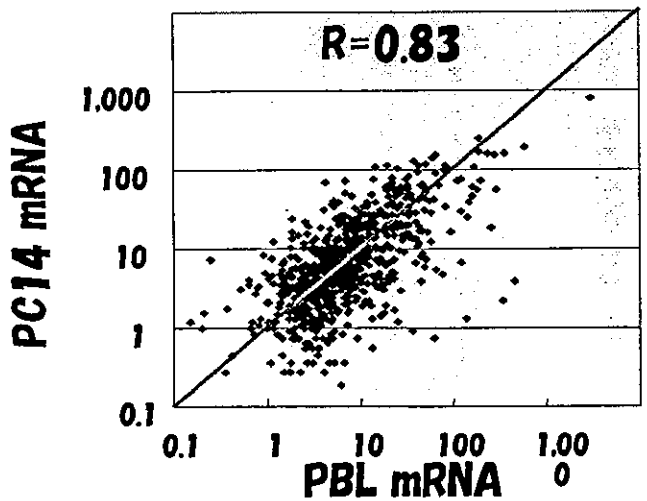


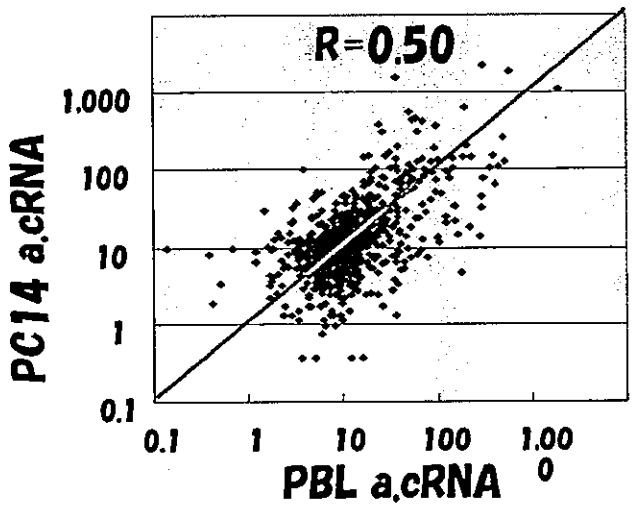

Fig 8

# Experimental design and drawing PBL samples (tissue sample)

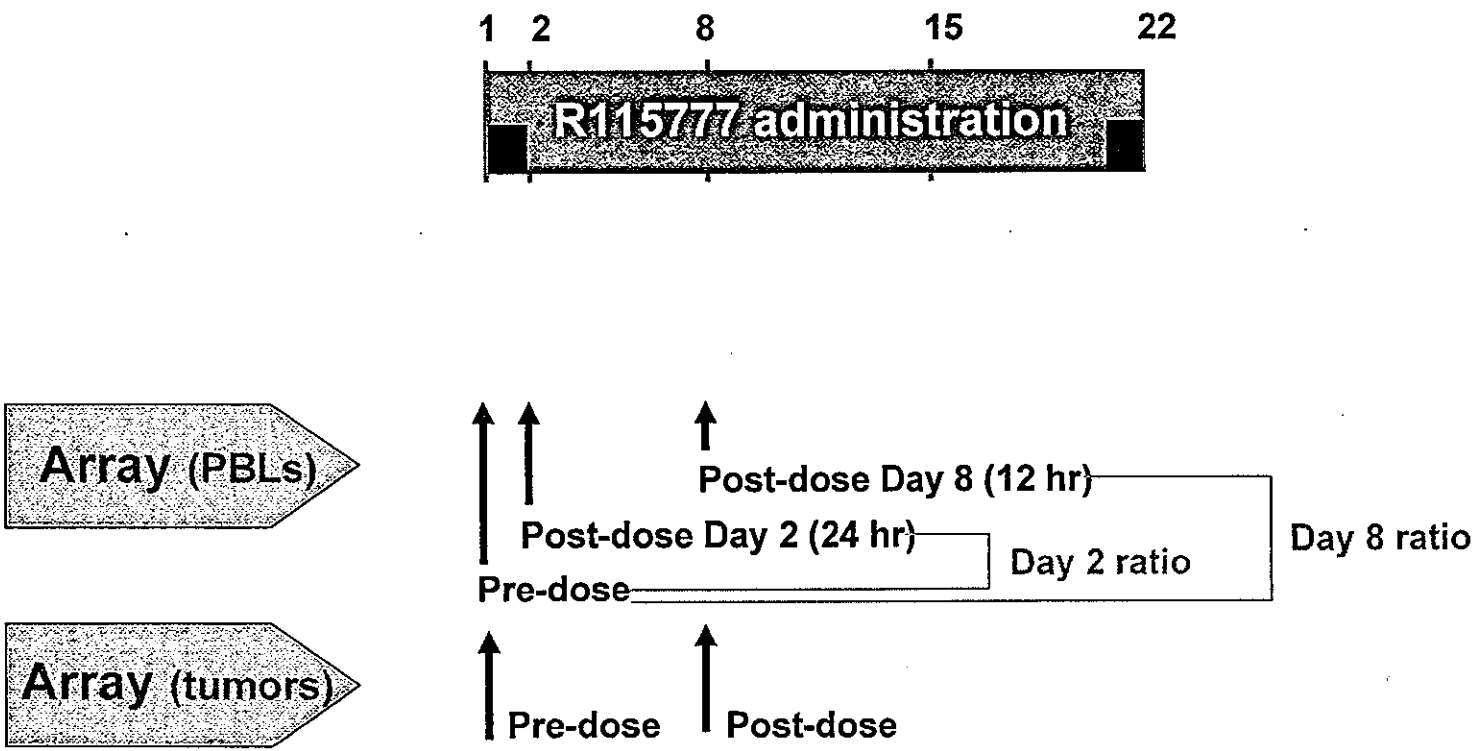

Fig.9 a

# Custom Atlas™ Array (cDNA filter-array)

*A set of 775 genes was chosen for predicting chemosensitivity analysis*



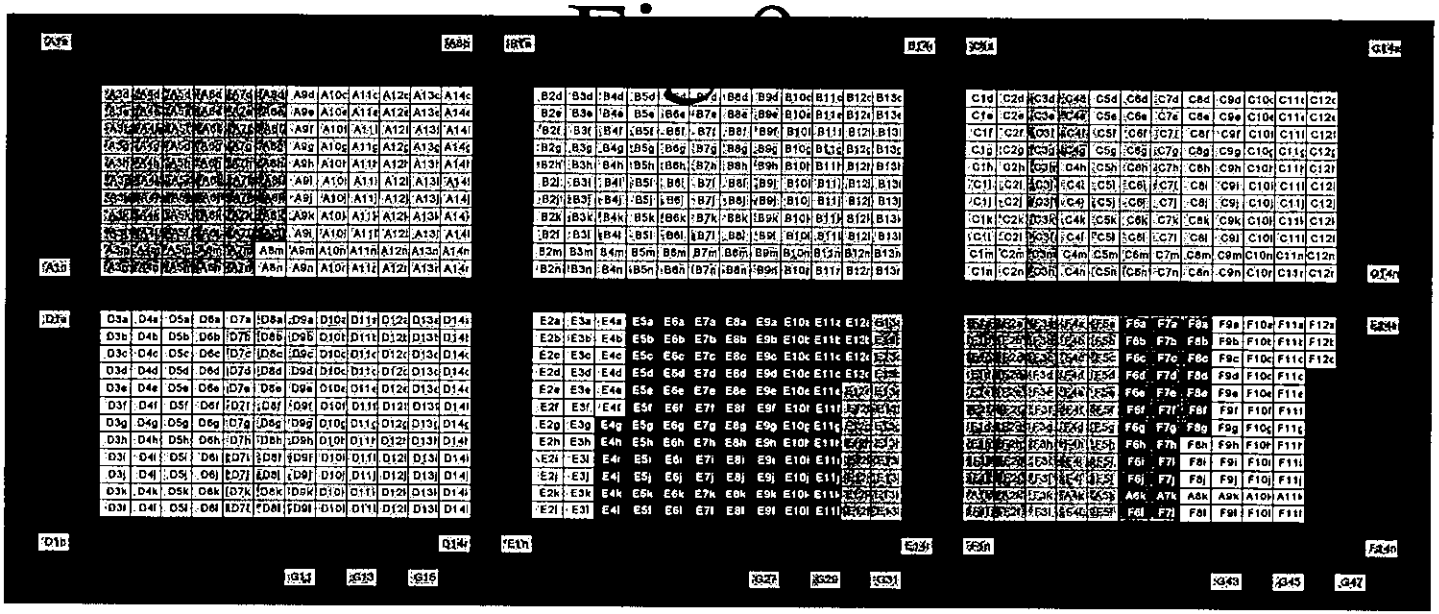

- 1: Cell Cycle Regulation
- 2: Signal / Oncogenes
- 3: Rho Family - Related Proteins
- 4: FTI - Related Proteins
- 5: Angiogenesis / Adhesion /Cell - Cell Interaction
- 6: Growth Factors
- 7: Cytokines
- 8: Apoptosis - Related Proteins
- 9: DNA Transcription Factors / Damage Response, Repair & Recombination
- 10: Metabolism
- 11: Translation / Protein Turnover / Detoxification Enzymes
- 12: Transporters / Nucleocytoplasmic Transporters / Symporters & Antiporters / Cytokeletal Proteins

*Produced by Pharmacology Division, National Cancer Center Research Institute, Tokyo, Japan*

Fig.9b



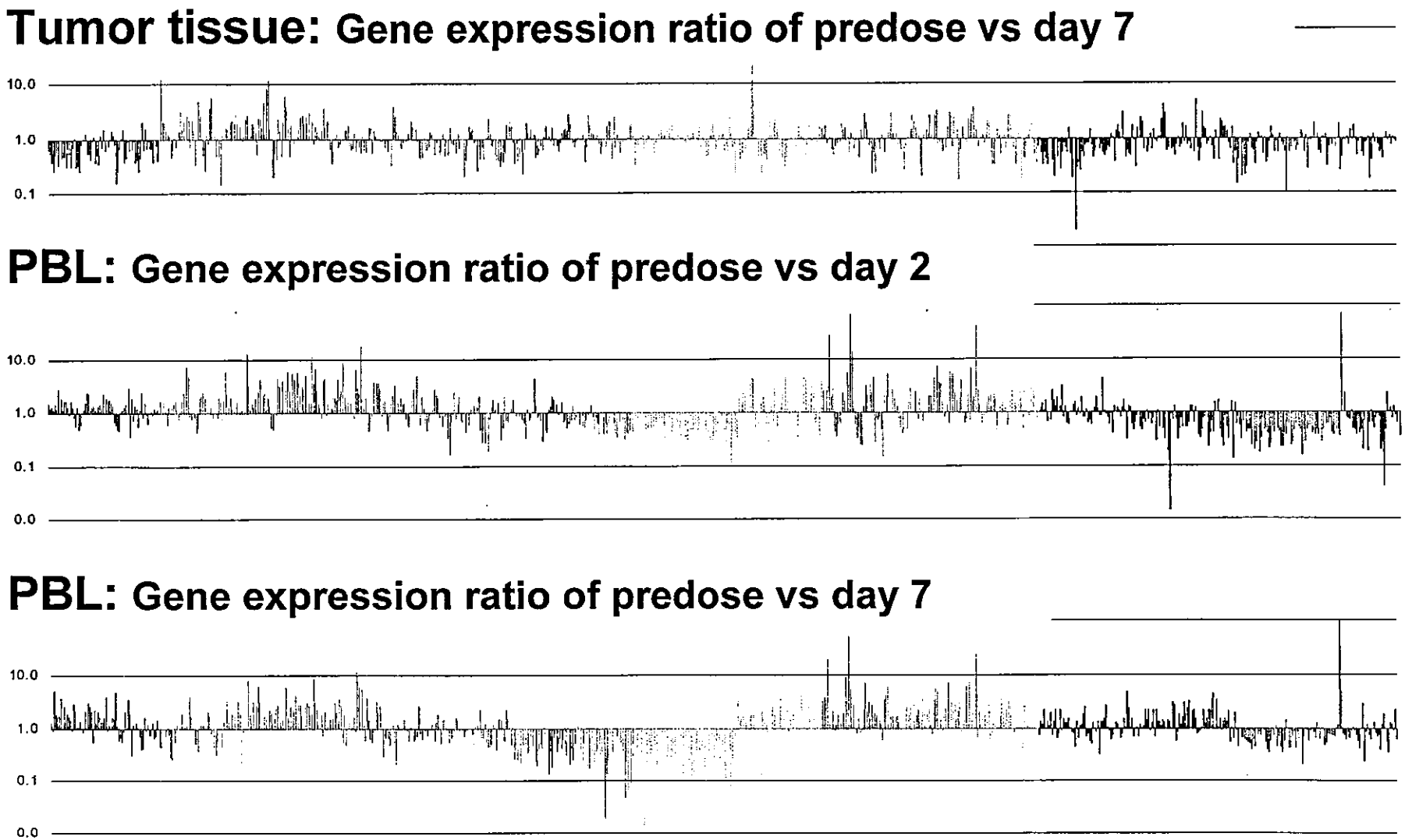
Tumor tissue: Gene expression ratio of predose vs day 7
10.0
1.0
0.1
PBL: Gene expression ratio of predose vs day 2
10.0
1.0
0.1
0.0
PBL: Gene expression ratio of predose vs day 7
10.0
1.0
0.1
0.0

*Int. J. Cancer:* **115**, 000–000 (2005)


# Establishment of a human non-small cell lung cancer cell line resistant to gefitinib

**Fumiaki Koizumi[1,3], Tatsu Shimoyama[1,4], Fumiko Taguchi[1,4], Nagahiro Saijo[2] and Kazuto Nishio[1,4]***
[1]*Shien-Lab, National Cancer Center Hospital, Tokyo, Japan*
[2]*Medical Oncology Department, National Cancer Center Hospital, Tokyo, Japan*
[3]*Investigative Treatment Division, National Cancer Center Institute EAST, Kashiwa, Japan*
[4]*Pharmacology Division, National Cancer Center Research Institute, Tokyo, Japan*

**The epidermal growth factor receptor (EGFR) tyrosine-kinase inhibitor gefitinib (Iressa™, ZD1839) has shown promising activity preclinically and clinically. Because comparative investigations of drug-resistant sublines with their parental cells are useful approaches to identifying the mechanism of gefitinib resistance and select factors that determine sensitivity to gefitinib, we established a human non-small cell lung carcinoma subline (PC-9/ZD) that is resistant to gefitinib. PC-9/ZD cells are ~180-fold more resistant to gefitinib than their parental PC-9 cells and PC-9/ZD cells do not exhibit cross-resistance to conventional anticancer agents or other tyrosine kinase inhibitors, except AG-1478, a specific inhibitor of EGFR. PC-9/ZD cells also display significant resistance to gefitinib in a tumor-bearing animal model. To elucidate the mechanism of resistance, we characterized PC-9/ZD cells. The basal level of EGFR in PC-9 and PC-9/ZD cells was comparable. A deletion mutation was identified within the kinase domain of EGFR in both PC-9 and PC-9/ZD, but no difference in the sequence of EGFR cDNA was detected in either cell line. Increased EGFR/HER2 (and EGFR/HER3) heterodimer formations were demonstrated in PC-9/ZD cells by chemical cross-linking and immunoprecipitation analysis in cells unexposed to gefitinib. Exposure to gefitinib increased heterodimer formation in PC-9 cells, but not in PC-9/ZD cells. Gefitinib inhibits EGFR autophosphorylation in a dose-dependent manner in PC-9 cells but not in PC-9/ZD cells. A marked difference in inhibition of site-specific phosphorylation of EGFR was observed at Tyr1068 compared to other tyrosine residues (Tyr845, 992 and 1045). To elucidate the downstream signaling in the PC9/ZD cellular machinery, complex formation between EGFR and its adaptor proteins Grb2, SOS, and Shc was examined. A marked reduction in the Grb2-EGFR complex and absence of SOS-EGFR were observed in PC-9/ZD cells, even though the protein levels of Grb2 and SOS in PC-9 and PC-9/ZD cells were comparable. Expression of phosphorylated AKT was increased in PC-9 cells and inhibited by 0.02 μM gefitinib. But the inhibition was not significant in PC-9/ZD cells. These results suggest that alterations of adaptor-protein-mediated signal transduction from EGFR to AKT is a possible mechanism of the resistance to gefitinib in PC-9/ZD cells. These phenotypes including EGFR–SOS complex and heterodimer formation of HER family members are potential biomarkers for predicting resistance to gefitinib.**
© *2005 Wiley-Liss, Inc.*

**Key words:** resistance; gefitinib; EGFR; Grb2; SOS; non-small cell lung cancer

Chemotherapy has played a central role in the treatment of patients with inoperable NSCLC for over 30 years, although its efficacy seems to be of very limited value.[1,2] Human solid tumors, including lung cancer, glioblastoma, breast cancer, prostate cancer, gastric cancer, ovarian cancer, cervical cancer and head and neck cancer, express epidermal growth factor receptor (EGFR) frequently, and elevated EGFR levels are related to disease progression, survival, stage and response to therapy.[2–10] The therapies directed at blocking EGFR function are attractive.

Interest in target-based therapy has been growing ever since the clinical efficacy of STI-571 was first demonstrated,[11–13] and small molecules and monoclonal antibodies that block activation of the EGFR and ErbB2 have been developed over the past few decades. The leading small-molecule EGFR tyrosine-kinase inhibitor, gefitinib (Iressa™, ZD1839), has shown excellent antitumor activity in a series of Phase I and II studies,[14,15] and Phase II international multicenter trials (IDEAL1 and 2) yield an overall RR of 11.8–18.4% and overall disease control rate of 42.2–54.4% (gefitinib 250 mg/day) in patients with advanced non-small cell lung cancer (NSCLC) who had undergo at least 2 previous treatments with chemotherapy. INTACT 1 and 2 ('Iressa' NSCLC Trials Assessing Combination Therapy) have demonstrated that gefitinib does not provide improvement in survival when added to standard first line platinum-based chemotherapy *vs.* chemotherapy alone in advanced NSCLC.[16,17] Two small retrospective studies reported recently that activating mutation of EGFR correlate with sensitivity and clinical response to gefitinib and erlotinib.[18–20] Although information of EGFR mutation may enable to identify the subgroup of patients with NSCLC who will respond to gefitinib and erlotinib, it would be expected that acquired resistance would develop in such patients after treatment. The problem of acquired resistance to gefitinib might be growing, but there has been no preclinical research about the mechanism of developing resistance to gefitinib. We established resistant subline using PC-9 that is highly sensitive to gefitinib.

Establishment of drug-resistant sublines and comparative investigations with their parental cells to identify their molecular, biological and biochemical properties are useful approaches to elucidating the mechanism of the drug's action. Our study describes the establishment of a gefitinib-resistant cell line and its characterization at the cellular and subcellular levels. The PC-9/ZD cell line is the first human NSCLC cell line resistant to gefitinib ever reported. PC-9 is a lung adenocarcinoma cell line that is highly sensitive to gefitinib at its $IC_{50}$-value of 0.039 μM, but the PC-9/ZD subline, which has a level of EGFR expression comparable to that of PC-9 cells, is specifically resistant to gefitinib. Thus, PC-9 and PC-9/ZD cells will provide useful information about the mechanism of developing resistance to gefitinib and molecules as surrogate markers for predicting chemosensitivity to gefitinib.



## Material and methods

### *Drugs and cells*

Gefitinib(*N*-(3-chloro-4-fluorophenyl)-7-methoxy-6-[3-(morpholin-4-yl)propoxy] quinazolin-4-amine) was supplied by AstraZeneca Pharmaceuticals (Cheshire, UK). AG-1478, AG-825, K252a, staurosporin, genistein, RG-14620 and Lavendustin A were purchased from Funakoshi Co. Ltd (Tokyo, Japan).

NSCLC cell line PC-9 (derived from a patient with adenocarcinoma untreated previously) was provided by Prof. Hayata of Tokyo Medical University (Tokyo, Japan).[21] PC-9 and PC-9/ZD cells were cultured in RPMI-1640 medium (Sigma, St. Louis, MO) supplemented with 10% FBS (GIBCO-BRL, Grand Island, NY), penicillin and streptomycin (100 U/ml and 100 μg/ml, respectively; GIBCO-BRL) in a humidified atmosphere of 5% $CO_2$ at 37°C. Gefitinib-resistant PC-9/ZD cells were selected from

***Correspondence to:** Shien-Lab, Medical Oncology Department, National Cancer Center Hospital, 5-1-1 Tsukiji, Chuo-ku, Tokyo, 104-0045, Japan. Fax: +81-3-3547-5185. E-mail: knishio@gan2.res.ncc.go.jp
Received 1 July 2004; Accepted after revision 21 December 2004
DOI 10.1002/ijc.20985
Published online 00 Month 2005 in Wiley InterScience (www.interscience.wiley.com).

J_ID: Z3Q Customer A_ID: 04-1248 Cadmus Art: IJC5519 Date: 22-FEBRUARY-05 Stage: I



a subculture that had acquired resistance to gefitinib using the following procedure. Cultured PC-9 cells were exposed to 2.5 μg/ml *N*-methyl-*N'*-nitro-*N*-nitrosoguanidine (MNNG) for 24 hr and then washed and cultured in medium containing 0.2 μM gefitinib for 7 days. After exposure to gefitinib, they were washed and cultured in drug-free medium for 14 days. When variable cells had increased, they were seeded in medium containing 0.3–0.5 μM of gefitinib on 96-well cultured plates for subcloning. After 21–28 days, the colonies were harvested and a single clone was obtained. The subcloned cells exhibited an 182-fold increase in resistance to the growth-inhibitory effect of gefitinib as determined by MTT assay, and the resistant phenotype has been stable for at least 6 months under drug-free conditions.

In vitro *growth-inhibition assay*

The growth-inhibitory effects of cisplatin, carboplatin, adriamycin, irinotecan, gemcitabine, vindesine, paclitaxel, genistein, K252a, staurosporin, AG-825, AG-1478, Tyrophostin 51, RG-14620, Lavendustin A and gefitinib in PC-9 and PC-9/ZD cells were examined by using a 3-(4,5-dimethylthiazol-2-yl)- 2,5-diphenyltetrazolium bromide (MTT) assay.[22] A 180 μl volume of an exponentially growing cell suspension ($6 \times 10^3$ cells/ml) was seeded into a 96-well microtiter plate, and 20 μl of various concentrations of each drug was added. After incubation for 72 hr at 37°C, 20 μl of MTT solution (5 mg/ml in PBS) was added to each well, and the plates were incubated for an additional 4 hr at 37°C. After centrifuging the plates at 200*g* for 5 min, the medium was aspirated from each well and 180 μl of DMSO was added to each well to dissolve the formazan. Optical density was measured at 562 and 630 nm with a Delta Soft ELISA analysis program interfaced with a Bio-Tek Microplate Reader (EL-340, Bio-Metallics, Princeton, NJ). Each experiment was carried out in 6 replicate wells for each drug concentration and carried out independently 3 or 4 times. The $IC_{50}$-value was defined as the concentration needed for a 50% reduction in the absorbance calculated based on the survival curves. Percent survival was calculated as: (mean absorbance of 6 replicate wells containing drugs − mean absorbance of six replicate background wells)/(mean absorbance of 6 replicate drug-free wells − mean absorbance of 6 replicate background wells) × 100.

In vivo *growth-inhibition assays*

Experiments were carried out in accordance with the United Kingdom Coordinating Committee on Cancer Research Guidelines for the welfare of animals in experimental neoplasia (2nd ed.). Female BALB/c nude mice, 6-weeks-old, were purchased from Japan Charles River Co. Ltd (Atsugi, Japan). All mice were maintained in our laboratory under specific-pathogen-free conditions. *In vivo* experiments were scheduled to evaluate the effect of oral administration of gefitinib on pre-existing tumors. Ten days before administration, $5 \times 10^6$ PC-9 or PC-9/ZD cells were injected subcutaneously (s.c.) into the back of the mice, and gefitinib (12.5, 25 or 50 mg/kg, p.o.) was administered to the mice on Days 1–21. Tumor diameter was measured with calipers on Days 1, 4, 8, 11, 14, 19 and 22 to evaluate the effect of treatment, and tumor volume was determined by using the following equation: tumor volume = $ab^2/2$ ($mm^3$) (where *a* is the longest diameter of the tumor and *b* is the shortest diameter). Day "x" denotes the day on which the effect of the drugs was estimated, and Day "1" denotes the first day of treatment. All mice were sacrificed on Day 22, after measuring their tumors. We considered absence of a tumor mass on Day 22 to indicate a cure. Differences in tumor sizes between the treatment groups and control group at Day 22 were analyzed by the unpaired *t*-test. A *p*-value of <0.05 was considered statistically significant.

*cDNA expression array*

The gene expression profile of PC-9/ZD was assessed with an Atlas Nylon cDNA Expression Array (BD Bioscience Clontech, Palo Alto, CA). Total RNA was extracted by a single-step guanidinium thiocyanate procedure (ISOGEN, Nippon Gene, Tokyo, Japan). An Atlas Pure Total RNA Labeling System was used to isolate RNA and label probes. The materials provided with the kit were used, and the manufacturer's instructions were followed for all steps. Briefly, streptavidin-coated magnetic beads and biotinylated oligo(dT) were used to isolate poly A RNA from 50 μg of total RNA and the RNA obtained was converted into $^{32}$P-labeled first-strand cDNA with MMLV reverse transcriptase. The $^{32}$P-labeled cDNA fraction was purified on NucleoSpin columns and was added to the membrane on which fragments of 777 genes were spotted. Hybridization was allowed to proceed overnight at 68°C. After washing, the radiolabeled spots were visualized and quantified by BAS-2000II and Array Gauge 1.1 (Fuji Film Co., Ltd., Tokyo, Japan). The data were adjusted for the total density level of each membrane.

*Quantitative Real-Time RT-PCR Analysis*

Total RNAs extracted from PC-9 cells and PC-9/ZD cells ($1 \times 10^6$ cells each) were incubated with DNase I (Invitrogen) for 30 min. First-strand cDNA synthesis was carried out on 1 μg of RNA in 10 μl of a reaction mixture with 50 pmol of Random hexamers and 50 U of M-MLV RTase. Oligonucleotide primers for human EGFR were obtained from Takara (HA003051, Takara Bio Co., Tokyo, Japan). For PCR calibration, we generated a calibrator dilution series for EGFR cDNA in pUSEamp vector (Upstate, Charlottesville, VA) ranging from $10^8$–$10^2$ copies/1 μl. A total of 2 μl of reverse transcriptase products was used for PCR amplification using Smart Cycler system (Takara) according to manufacturer's instructions. Absolute copy numbers were calculated back to the initial cell numbers, which were set into the RNA extraction. As a result we obtained copies/cell:ratio representing the average EGFR RNA amount per cell. AQ3

*Immunoprecipitation and immunoblotting*

The cultured cells were washed twice with ice-cold PBS, and lysed in EBC buffer (50 mM Tris-HCl, pH 8.0, 120 mM NaCl, 0.5% Nonidet P-40, 100 mM NaF, 200 mM Na orthovanadate, and 10 mg/ml each of leupeptin, aprotinin, pepstatin A and phenylmethylsulphonyl fluoride). The lysate was cleared by centrifugation at 15,000 r.p.m. for 10 min, and the protein concentration of the supernatant was measured by BCA protein assay (Pierce, Rockford, IL). The membrane was probed with antibody against EGFR (1005; Santa Cruz, Santa Cruz, CA), HER2/neu (c-18; Santa Cruz), HER3 (c-17; Santa Cruz), HER4 (c-18; Santa Cruz), PI3K (4; BD), Grb2 (81; BD), SOS1/2 (D-21; Santa Cruz), Shc (30; BD; San Jose, CA), PTEN (9552; Cell Signaling, Beverly, MA), AKT (9272; Cell Signaling), phospho-EGFR specific for Tyr 845, Tyr 992, Tyr 1045, and Tyr 1068 (2231, 2235, 2237, 2234; Cell Signaling), phospho-AKT (Ser473) (9271; Cell Signaling), phospho-Erk (9106; Cell Signaling), and phospho-Tyr (PY-20; BD) as the first antibody, and then with by horseradish-peroxidase-conjugated secondary antibody. The bands were visualized by enhanced chemiluminescence (ECL Western Blotting Detection Kit, Amersham, Piscataway, NJ). For Immunoprecipitation, $5 \times 10^6$ cells were washed, lysed in EBC buffer, and centrifuged, and the supernatants obtained (1,500 μg) were incubated at 4°C with the anti-EGFR (1005), -HER2 (c-18), and -HER3 (c-17) Ab overnight. The immunocomplexes were absorbed onto protein A/G-Sepharose beads, washed 5 times with lysate buffer, denatured, and subjected to electrophoresis on a 7.5% polyacrylamide gel.

*Analysis of the genes of the HER families by direct sequencing*

Total RNAs were extracted from PC-9 and PC-9/ZD cells with ISOGEN (Nippon Gene) according to manufacturer's instructions. First-strand cDNA was synthesized from 2 μg of total RNA by using 400 U of SuperScript II (Invitrogen, Carlsbad, CA). After reverse transcription with oligo (dT) primer (Invitrogen) or random primer (Invitrogen), the first-strand cDNA was amplified by PCR by using specific primers for EGFR, HER2 and HER3. The

J_ID: Z3Q Customer A_ID: 04-1248 Cadmus Art: IJC5519 Date: 22-FEBRUARY-05 Stage: I



reaction mixture (50 μl) contained 1.25 U AmpliTaq DNA polymerase (Applied Biosystem, Foster City, CA), and amplification was carried out by 30 cycles of denaturation (95°C, 30 sec), annealing (55–59°C, 30 sec), and extension (72°C, 30 sec) with a GeneAmp PCR System 9600 (Applied Biosystem). After amplification, 5 μl of the RT-PCR products was subjected to electrophoretic analysis on a 2% agarose gel with ethidium bromide. DNA sequencing of the PCR products was carried out by the dideoxy chain termination method using the ABI PRISM 310 Genetic Analyzer (Applied Biosystem).

*Chemical cross-linking*

Chemical cross-linking in intact cells was carried out as described previously.[23] In brief, after 6 hr exposure to 0.2 μM gefitinib, cells were washed with PBS and incubated for 25 min at 4°C in PBS containing 1.5 mM of the nonpermeable cross-linker bis (sulfosuccinimidyl) substrate (Pierce, Rockford, IL). The reaction was terminated by adding 250 mM glycine for 5 min while rocking. Cells were washed in EBC buffer and 20 μg of protein was resolved by 5–10% gradient SDS-PAGE, and then immunoblot analyzed for EGFR, HER2, HER3 and P-Tyr.

## Results

*Sensitivity of PC-9/ZD cells to cytotoxic agents and tyrosine kinase inhibitors*

No significant difference between PC-9 and PC-9/ZD cells was observed in *in vitro* cell growth (doubling time of 20.3 hr and 21.4 hr, respectively) and microscopic morphology. Figure 1 shows the growth-inhibitory effect of gefitinib on the parent PC-9 cell line and its resistant subline, PC-9/ZD. The $IC_{50}$-value of gefitinib in PC-9 cells was 0.039 μM, as compared to 7.1 μM in PC-9/ZD cells (182-fold resistance). PC-9/ZD cells exhibited no cross-resistance to other conventional anticancer agents, including cisplatin, carboplatin, adriamycin, vindesine, paclitaxel and irinotecan. We also examined the growth-inhibitory effect of the EGFR tyrosine kinase inhibitors AG-1478, RG-14620 and Lavendustin A and other tyrosine kinase inhibitors in PC-9 and PC-9/ZD cells. PC-9/ZD cells show cross-resistance to AG1478, but not to all of the tyrosine kinase inhibitors (Tables I, II). It is likely that PC-9/ZD would also be resistant to EGFR-targeted quinazoline derivatives including gefitinib and erlotinib.[20]

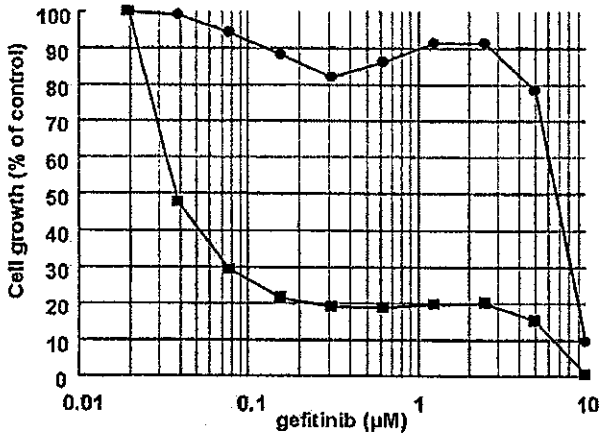


| | PC-9 | PC-9/ZD |
|---|---|---|
| $IC_{50}$ value (μM) | 0.039 ± 0.002 | 7.1 ± 0.06 |
| Doubling time (hr) | 20.3 | 21.0 |

FIGURE 1 – Growth-inhibitory effect of gefitinib on PC-9 and PC-9/ZD cells determined by MTT assay. The cells were exposed to the concentrations of gefitinib indicated for 72 hr. The growth-inhibition curves of PC-9 (■) and PC-9/ZD (●) are shown. Doubling time was determined by MTT assay.

TABLE I – CHEMOSENSITIVITY TO OTHER ANTICANCER DRUGS

| Drug | $IC_{50}$ values (μM)[1] | | RR[2] 1.6 |
|---|---|---|---|
| | PC-9 | PC-9/ZD | |
| Cisplatin | 1.9 ± 0.7 | 3.1 ± 1.5 | 2.0 |
| Carboplatin | 25 ± 21 | 49 ± 23 | 1.3 |
| Adriamycin | 0.16 ± 0.13 | 0.20 ± 0.15 | 2.2 |
| Irinotecan | 15 ± 10 | 32 ± 11 | 1.5 |
| Etoposide | 4.5 ± 1.5 | 6.6 ± 1.3 | 1.5 |
| Gemcitabine | 18 ± 1.5 | 27 ± 1.5 | 0.7 |
| Vindesine | 0.0046 ± 0.0004 | 0.0032 ± 0.0009 | 1.2 |
| Paclitaxel | 0.0041 ± 0.0011 | 0.0048 ± 0.0004 | 1.6 |

[1]As assessed by MTT assay in PC-9 and PC-9/ZD cells. Values are the mean ± SD of >3 independent experiments.–[2]Relative resistance value ($IC_{50}$ of resistant cells/$IC_{50}$ of parental cells).

*PC-9/ZD cells show significant resistance to gefitinib in an in vivo model*

To ascertain whether the resistance of PC-9/ZD occurs *in vivo*, we investigated the growth-inhibitory effect of gefitinib on PC-9 cells and PC-9/ZD cells in a xenotransplanted model. There was no significant difference in the size of the of PC-9 and PC-9/ZD cell tumor masses in nude mice before the start of gefitinib injection. Figure 2 shows the growth-inhibition curve of PC-9 (Fig. 2*a*) and PC-9/ZD (Fig. 2*b*) cells *in vivo* during the observation period. The PC-9 tumor masses decreased markedly in volume at all doses of gefitinib. In the 50 mg/kg/day p.o. group, the PC-9 masses were eradicated in all mice and did not regrow within the observation period. Growth of the PC-9/ZD masses, on the other hand, was inhibited by gefitinib administration in a dose-dependent manner, but significant tumor reduction was observed only in the 25 and 50 mg/kg/day groups, and the PC-9/ZD masses were not eradicated even in 50 mg/kg/day group. These results clearly demonstrate the significant *in vivo* resistance of PC-9/ZD cells to gefitinib.

*Expression of HER family members and related molecules in PC-9 and PC-9/ZD cells*

We examined the gene expression and protein levels of HER family members and related molecules by cDNA expression array (followed by confirmation using RT-PCR, data not shown) and immunoblotting. The ratios of the protein expression levels of PC-9 cells to PC-9/ZD cells almost paralleled the expression levels of their genes (Fig. 3*a*). The basal level of EGFR was comparable or slightly higher in PC-9/ZD cells (Fig. 3*a*,*b*), whereas the HER3 and AKT levels were lower in resistant cells.

We carried out quantitative RT-PCR to measure the copy numbers of EGFR. Estimated transcript levels of EGFR were 786.3 and 712.1 copies/cell for PC-9 cells and PC-9/ZD cells, respectively (Fig. 3*d*). Relative ratio of EGFR expression levels in PC-9 cells and PC-9/ZD cells is 1.104. Microarray analysis using CodeLink Bioarray (Amersham Bio, Piscataway, NJ) confirmed equivalent gene expression of EGFR with ratio of 1.002 between PC-9 and PC-9/ZD cells (data not shown).

Expression of PI3K, Grb2, SOS, and Shc, the adaptor proteins of EGFR, and PTEN was almost the same in PC-9 and PC-9/ZD cells, and no change in the protein levels was observed after exposure to gefitinib (data not shown). The relative densitometric units of each protein are shown in Figure 3*c*. These results suggest that the difference in protein levels of EGFR, HER2, and related proteins can not explain the high resistance of PC-9/ZD cells to gefitinib.

*Sequence of HER family member in PC-9/ZD cells*

Several reports suggest that the resistance to receptor tyrosine kinase inhibitor STI-571 is partially due to mutations in the

J_ID: Z3Q Customer A_ID: 04-1248 Cadmus Art: IJC5519 Date: 22-FEBRUARY-05 Stage: I



TABLE II – CHEMOSENSITIVITY TO PROTEIN KINASE INHIBITORS[1]

| Inhibitor | Target | $IC_{50}$ values (μM) | | RR[2] |
|---|---|---|---|---|
| | | PC-9 | PC-9/ZD | |
| AG-1478 | EGFR | 0.052 ± 0.02 | 6.0 ± 0.8 | 117 |
| RG-14620 | EGFR | 13 ± 1.0 | 13 ± 2.5 | 1.0 |
| Lavendustin A | EGFR | 20 ± 4.6 | 27 ± 2.6 | 1.3 |
| Genistein | TK | 18 ± 1.5 | 27 ± 1.5 | 1.5 |
| K252a | PKC | 0.47 ± 0.17 | 0.63 ± 0.04 | 1.3 |
| Staurosporin | PKC | 0.0036 ± 0.0019 | 0.004 ± 0.0014 | 1.1 |
| AG-825 | HER2 | >50 | >50 | |

[1]Assessed by MTT assay in PC-9 and PC-9/ZD cells. Values are the mean ± SD of >3 independent experiments.–[2]Relative resistance value ($IC_{50}$ of resistant cells/$IC_{50}$ of parental cells).

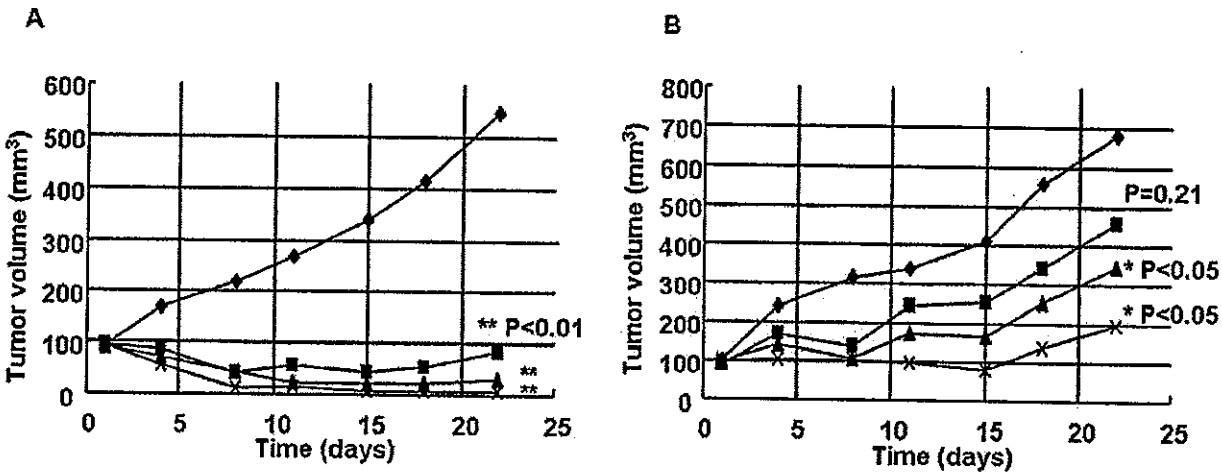


FIGURE 2 – Growth-inhibitory effect of gefitinib on PC-9 and PC-9/ZD cells xenotransplanted into nude mice. Ten days before gefitinib administration, $5 \times 10^6$ PC-9 (*a*) or PC-9/ZD (*b*) cells were injected s.c. into the back of mice. The mice were divided into 4 groups (◆, control group; ■, 12.5 mg/Kg group; ▲, 25 mg/Kg group; ×, 50 mg/Kg group). Gefitinib was administered p.o. to the tumor-inoculated mice on Days 1–21. Each group consisted of 6 mice. The statistical analysis was carried out by using the unpaired *t*-test.

ATP-binding site of the Bcr-Abl, the target of the drug.[24–27] We analyzed the sequences of the cDNAs of EGFR, HER2, and HER3, but found no differences in their sequences between PC-9 and PC-9/ZD cells. We did detect a deleted position of EGFR in both cell lines that results in deletion of 5 amino acids (Glu722, Leu723, Arg724, Glu725, and Ala726) (Fig. 4). Our findings indicate that the deletion does not directly contribute to the cellular resistance.

F4

*Inhibitory effect of gefitinib on autophosphorylation of EGFR in PC-9/ZD cells*

Phosphorylation of EGFR is necessary for EGFR-mediated intracellular signaling. Although the EGFR phosphorylation levels of tumors were thought to be correlated with sensitivity to gefitinib, the basal level of phosphorylated EGFR in PC-9 and PC-9/ZD cells is almost the same. Gefitinib inhibited EGFR autophosphorylation in a dose-dependent manner and completely inhibited its phosphorylation at 0.2–2 μM in PC-9 cells (Fig. 5*a*), but its inhibitory effect on autophosphorylation of EGFR in PC-9/ZD cells was less than in PC-9 cells (Fig. 5*a*). Because each phosphorylation site of EGFR has a different role in the activation of downstream signaling molecules, we examined the inhibitory effect of gefitinib on site-specific phosphorylation of EGFR. Phosphorylation of several different EGFR tyrosine residues (Tyr845, Tyr992 and Tyr1068) was dose-dependently inhibited by gefitinib in PC-9 cells, whereas no clear inhibitory effects of gefitinib on phosphorylation at Tyr 845 and Tyr1068 residues in PC-9/ZD cells was observed (Fig. 5*b,c,e*). The most marked difference of in inhibition between the cells was observed at Tyr1068 (Fig. 5*e*). Tyr1045 showed resistance to inhibition of autophosphorylation by gefitinib in both PC-9 and PC-9/ZD cells (Fig. 5*d*).

F5

*Complex formation of EGFR and its adaptor proteins*

Tyr1068 of EGFR is the tyrosine that is most resistant to inhibition of autophosphorylation by gefitinib in PC-9/ZD cells. Because the Tyr 1068 is a direct binding site for the Grb2/SH2 domain, and its phosphorylation is related to the complex formation of EGFR-adaptor proteins and their signaling, we examined complex formation between EGFR and the adaptor proteins GRB2, SOS, Shc, and PI3K by immunoprecipitation. The level of expression of these proteins in PC-9 and PC-9/ZD cells were similar (Fig. 3*a*). A smaller amount of EGFR-GRB2 complex was observed in PC-9/ZD cells and no EGFR-SOS complex was detected at all (Fig. 6). The amount of HER2- or HER3-GRB2 complex in PC-9 and PC-9/ZD cells was similar, and no decreases in complex formation were observed after exposure to gefitinib. A decreased amount of HER2-SOS complex and inability to detect HER3-SOS complex were also observed in PC-9/ZD cells. HER2-PI3K complex increased in PC-9/ZD. There are no significant differences in complex formation between SHC and EGFR, HER2, or HER3 between PC-9 and PC-9/ZD cells. These results suggest that Grb2-SOS-mediated signaling may be inactivated in PC-9/ZD cells.

F6

*Heterodimerization of HER family member in PC-9/ZD cells*

Dimerization of members of the HER family is essential for activation of their catalytic activity and their signaling. We examined the effect of gefitinib on the dimerization of HER family members by immunoblotting, immunoprecipitation and chemical cross-linking analysis (Figs. 3*a*, 5*a*, 7*a*). The expression levels of EGFR and HER2 were similar and the HER3 level was lower in PC-9/ZD cells by immunoblotting (Fig. 3*a*). A chemical cross-

F7

J_ID: Z3Q Customer A_ID: 04-1248 Cadmus Art: IJC5519 Date: 22-FEBRUARY-05 Stage: I



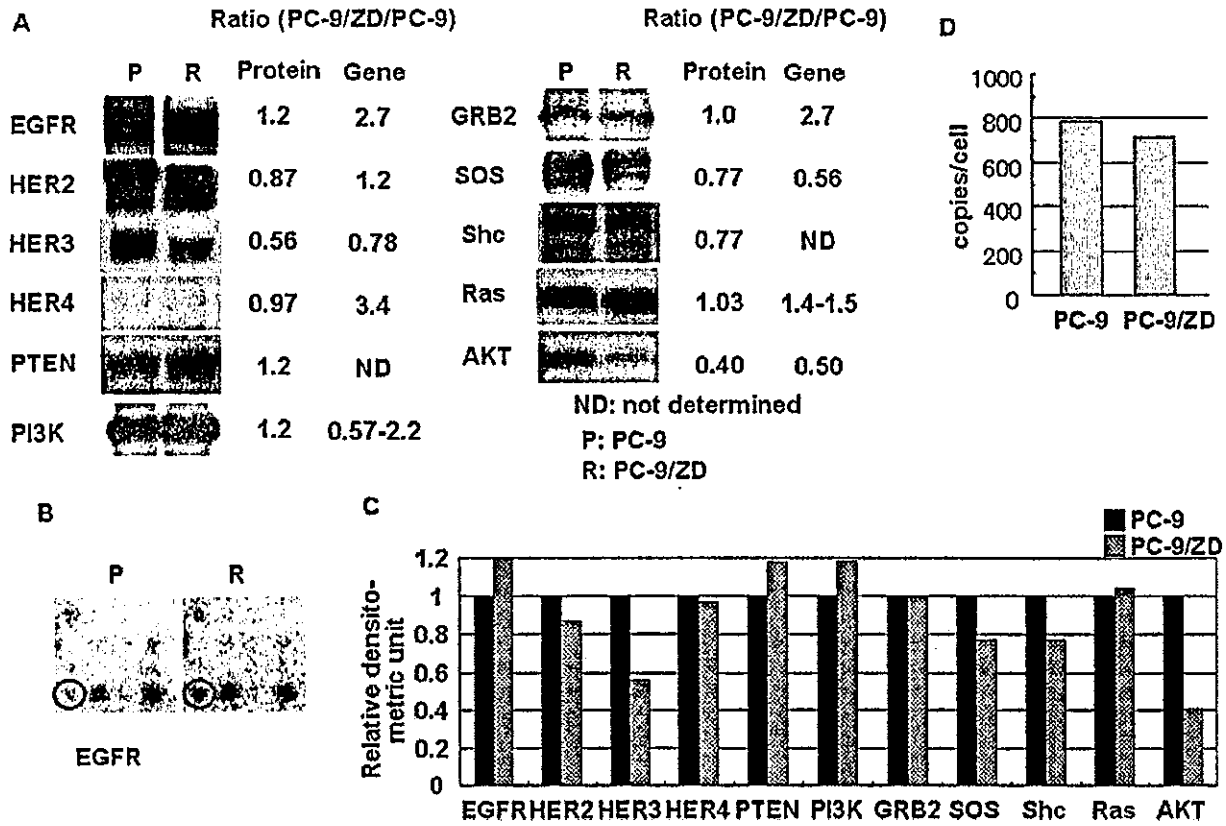


FIGURE 3 – Expresssion of HER family members and related molecules in PC-9 (P) and PC-9/ZD (R) cells. (*a*) Western blot analysis; a 20 μg sample of total cell lysates was separated by SDS-PAGE, transferred to a PVDF membrane, and incubated with a specific anti-human antibody as the first antibody and then with horseradish peroxidase-conjugated secondary antibody. The ratios of the levels of expression of proteins and genes in PC-9 cells to the levels in PC-9/ZD cells are shown. (*b*) cDNA expression array; Poly A RNA was converted into $^{32}$P-labeled first-strand cDNA with MMLV reverse transcriptase. The $^{32}$P-labeled cDNA fraction was hybridized to the membrane on which fragments of 777 genes were spotted. The close-up view shows EGFR mRNA expression. (*c*) Each band was quantified by a densitometry and with NIH image software. The levels of protein expression are shown in a graph. (*d*) Absolute amounts of EGFR transcripts of PC-9 cells and PC-9/ZD cells measured by real-time quantitative RT-PCR. The values were calculated back to the initial cell numbers for RNA extraction in Material and Methods.

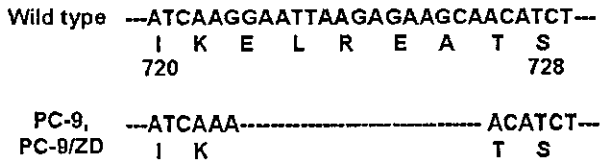


FIGURE 4 – Detection of a deleted position of EGFR. Direct sequencing of a PC-9 and PC-9/ZD-derived, amplified cDNA fragment containing the ATP-binding site of EGFR. *Top*, wild-type EGFR; *bottom*, PC-9 and PC-9/ZD.

linking assay showed that in the absence of gefitinib the amount of high molecular weight complexes (~400 kDa) that are recognized by anti-EGFR antibody (EGFR dimers), including formations of homodimers and heterodimers (EGFR-EGFR, EGFR-HER2 or EGFR-HER3), was almost the same in PC-9 and PC-9/ZD cells, whereas HER2 dimerization detected by anti-HER2 antibody was remarkably lower in PC-9/ZD cells (Fig. 7*a*). Increased EGFR/HER2 (and EGFR/HER3) heterodimer formation was detected in PC-9/ZD cells by immunoprecipitation analysis (Fig. 5*a*). The proportion of EGFR heterodimer to homodimer is increased significantly in PC-9/ZD (Fig. 7*b*). When exposed to gefitinib at a concentration of 0.2 μM for 6 hr the amount of dimer-formation increased similarly in PC-9 and PC-9/ZD cells (Fig. 7*a*), whereas marked induction of hetero-dimerization of EGFR-HER2 was observed only in PC-9 cells (Fig. 5*a*). These results suggest that a difference in hetero- or homo-dimerization is a possible determinant factor of gefitinib sensitivity.

*AKT and MAPK pathways in PC-9/ZD cells*

Because phosphorylation at Tyr 1068 of EGFR plays an important role for transduction of the signal to downstream of MAPK and AKT pathway,[28,29] we examined the difference between PC-9 and PC-9/ZD cells in downstream signaling. The basal level of phosphorylated AKT is higher in PC-9 cells than in PC-9/ZD cells, and although gefitinib inhibited AKT phosphorylation in a dose-dependent manner (Fig. 9*a*), the inhibitory effect of gefitinib on phosphorylation of AKT in PC-9/ZD cells was significantly less than in PC-9 cells (Fig. 9*a*). This difference in the inhibitory effect of gefitinib on AKT phosphorylation between PC-9 and PC-9/ZD cells is very similar to the difference in effect on EGFR autophosphorylation. No inhibition of phosphorylation of MAPK by gefitinib was observed in either cell line (Fig. 9*b*). These results suggest that downregulation of activated AKT is closely correlated with the cellular sensitivity to gefitinib, but that inhibition of the MAPK pathway does not contribute to drug sensitivity.

AQ4

J_ID: Z3Q Customer A_ID: 04-1248 Cadmus Art: IJC5519 Date: 22-FEBRUARY-05 Stage: I



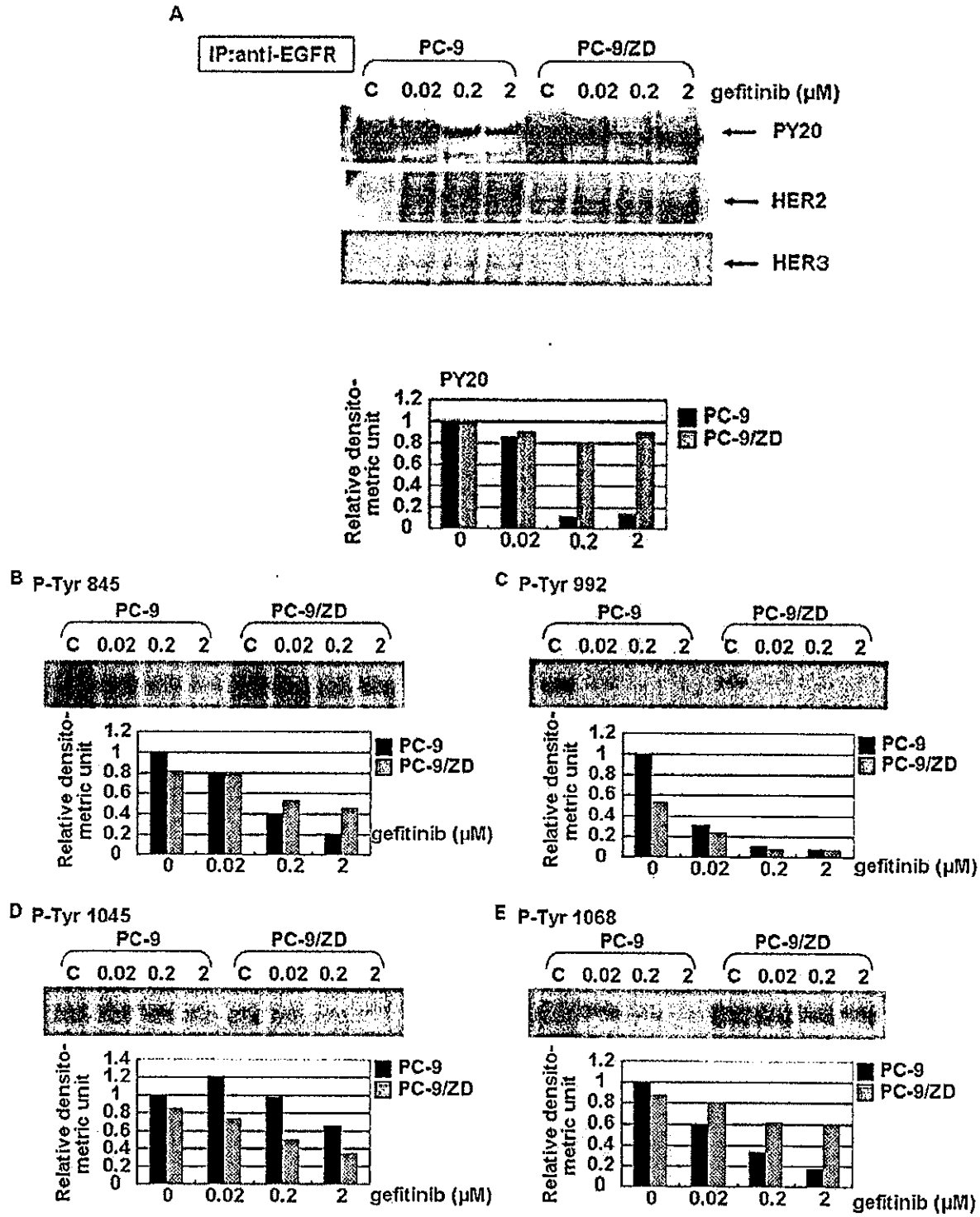


FIGURE 5 – Effect of gefitinib on autophosphorylation of EGFR. (*a*) PC-9 and PC-9/ZD cells ($5 \times 10^6$) were exposed to 0.02, 0.2 or 2 μM gefitinib for 6 hr. The 1,500 μg of total cell lysate was immunoprecipitated with an anti-EGFR antibody. The immunoprecipitates were subjected to gel electrophoresis and Western blotting with anti-phosphotyrosine, anti-HER2 and anti-HER3 antibodies. Tyrosine-phosphorylated EGFR was determined with an anti-phosphotyrosine antibody. Heterodimer formation of EGFR was analyzed with anti-HER2 and anti-HER3 antibodies. The expression levels have been plotted in a graph. (*b–e*) PC-9 and PC-9/ZD cells were exposed to 0.02, 0.2 and 2 μM gefitinib for 6 hr. A 20 μg of protein of each sample was analyzed by Western blotting by using anti phospho-EGFR (Tyr845, Tyr992, Tyr 1045, Tyr 1068) antibodies.

J_ID: Z3Q Customer A_ID: 04-1248 Cadmus Art: IJC5519 Date: 22-FEBRUARY-05 Stage: I



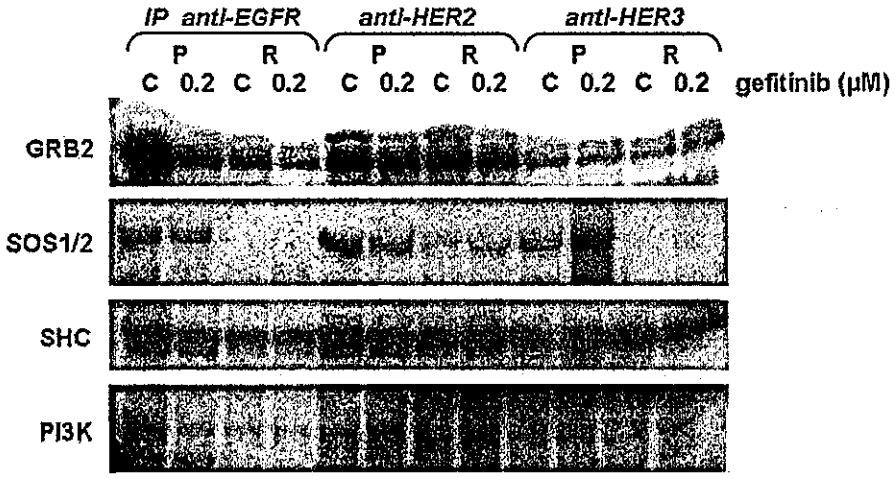


FIGURE 6 – Protein interaction between EGFR and its adaptor proteins. Cells (P: PC-9, R: PC-9/ZD) were exposed to 0 and 0.2 μM of gefitinib for 6 hr. The cells were lysed and immunoprecipitated with ant-EGFR, anti-HER2, and anti-HER3 antibodies, and the amounts of the Grb2, SOS1/2, SHC and PI3K precipitated were monitored by immunoblotting with their specific Abs.

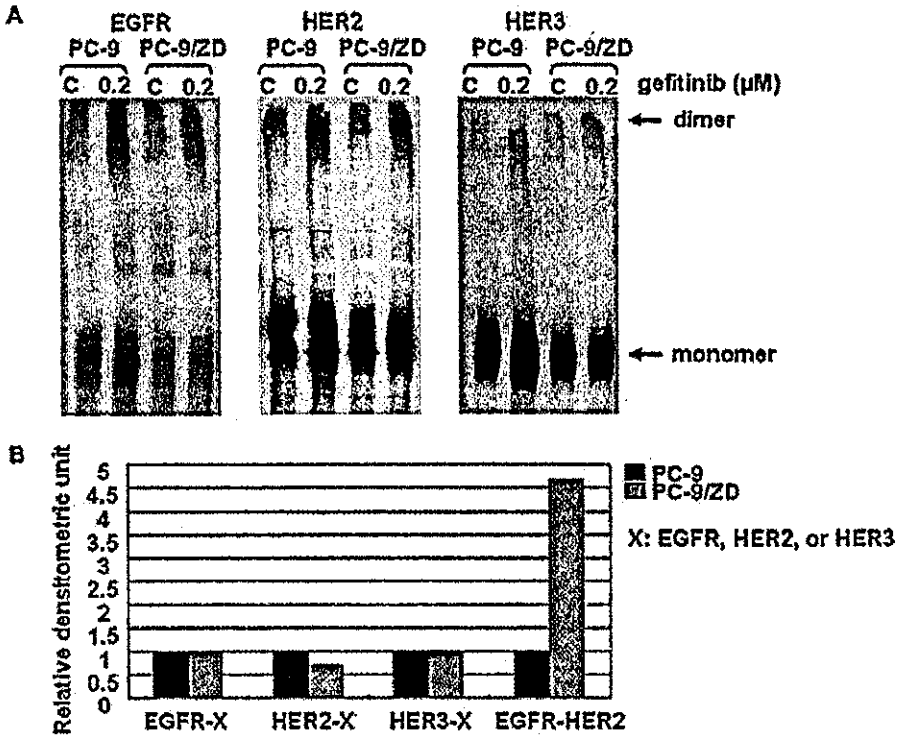


FIGURE 7 – Chemical cross-linking of PC-9 and PC-9/ZD cells. (*a*) After 6 hr exposure to 1.5 mM bis (sulfosuccinimidyl) substrate dissolved in PBS as indicated in Material and Methods. The cross-linking reaction was quenched and the cell lysates were prepared and subjected to immunoblot analysis of EGFR, HER2 and HER3. (*b*) Ratio of dimmers formed by PC-9 cells to those by PC-9/ZD cells in the absence of gefitinib. The density of the bands in (*a*) for EGFR-X, HER2-X and HER3-X were quantified densitometrically. The ratio of EGFR-HER2 was calculated by the band density obtained in Figure 5*a*. X = EGFR, HER2 or HER3.

## Discussion

Interest in resistance to target-based therapy (TBT) has been growing ever since clinical efficacy was first demonstrated.[11–13] Although CML patients respond to STI-571 well at first, most patients eventually relapse in the late stage of the disease.[25–27] It has been reported that some patients in whom treatment with gefitinib is effective at first, ultimately become refractory.[30] Resistance is likely to remain a hurdle that limits the long-term effectiveness of TBT. PC-9 had a deletion mutation within the kinase domain of EGFR and is highly sensitive. These characters are similar to those of NSCLC with clinical responsiveness to gefitinib. Analyzing the mechanism of resistance of PC-9/ZD subline might be clinically meaningful.

The mechanism of drug resistance is thought to be multifactorial. Because the growth-inhibitory assay in our present study showed no cross resistance to a variety of cytotoxic agents, the mechanism of the resistance differs from the mechanism of multidrug resistance patterns. Although expression of BCRP, one of the multidrug-resistance-related proteins has been reported to contribute to the resistance to gefitinib,[31] expression of BCRP mRNA is observed only in PC-9 cells (data not shown). Although mutations in the ATP-binding pocket of BCR-ABL gene have been identified recently in cells from CML patients who were refractory to STI-571 treatment or relapse,[25–27] there have been no reports of any such mutations for gefitinib resistance. PC-9/ZD also became refractory to gefitinib without secondary mutation in EGFR cDNA. These suggest the possibility of refractory tumor after treatment of gefitinib including this kind of phenotype.

There is no significant difference in expression level of EGFR between PC-9 and PC-9/ZD. Does the antitumor effect of gefitinib

J_ID: Z3Q Customer A_ID: 04-1248 Cadmus Art: IJC5519 Date: 22-FEBRUARY-05 Stage: I



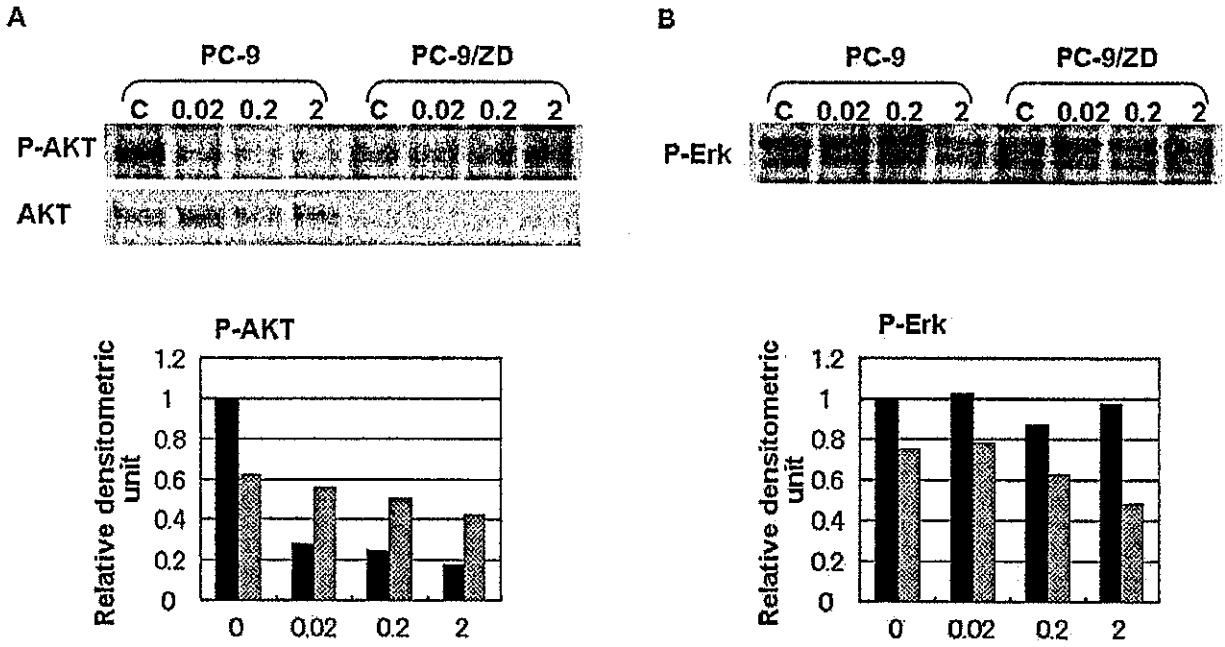


FIGURE 8 – Effect of gefitinib on the MAPK and AKT pathway. Cells were placed in medium containing 0, 0.02, 0.2 or 2 μM of gefitinib for 6 hr and harvested in EBC buffer. Total cellular lysates were separated on SDS-PAGE, transferred to a membrane and blotted with (*a*) anti-phospho-AKT (Ser473) and (*b*) anti-phospho-Erk (p44/42) antibodies. The expression levels are shown in a graph.

require EGFR expression? Naruse *et al.*[32] suggested that the high sensitivity of K562/TPA to gefitinib is due to acquired EGFR expression. In their study autophosphorylation of EGFR in K562/TPA cells was inhibited by 0.01 μM gefitinib, and the $IC_{50}$-value of gefitinib in parental K562 cells, which do not express EGFR, was approximately 400-fold higher than that in the K562/TPA subline. Furthermore, most patients who responded to gefitinib therapy have EGFR mutation in lung tumor.[18,19] These findings suggest strongly that gefitinib exerts its antitumor effect through an action on EGFR. Our present study showed similar EGFR expression and autophosphorylation levels in PC-9 and PC-9/ZD cells. The inhibitory effect of gefitinib on phosphorylation of EGFR is different. PC-9/ZD did not show cross-resistance to the specific EGFR TK inhibitors RG-14620 and Lavendustin A in an MTT assay, nor did inhibit the phosphorylation of EGFR at the cellular level (data not shown). Paez *et al.*[18] reported that phosphorylation of EGFR in gefitinib-resistant cell lines was inhibited only when gefitinib was present at high concentration. These findings suggest that the difference in the inhibitory-effect on EGFR phosphorylation may determine the efficacy of the drug.

The inhibitory effect of gefitinib on EGFR phosphorylation is not significant in PC-9/ZD cells despite the absence of differences in the sequences of EGFR, HER2, and HER3. There are several possible explanations for the difference in inhibitory effect. First, the avidity of gefitinib for the ATP-binding site of EGFR may be decreased in PC-9/ZD cells due to a protein-protein interaction, *i.e.*, EGFR and a certain protein prevent gefitinib from binding to EGFR. Second, a change in the activity of specific protein-tyrosine kinase or phosphatase of EGFR in PC-9/ZD cells, especially after exposure to gefitinib, may result in resistance to inhibition of EGFR phosphorylation. The phosphorylation level is maintained in exquisite balance by the reciprocal activities of kinase and phosphatase,[33,34] and Wu reported that phosphatase plays a role in STI571-resistance.[35] Third, increased heterodimer formation by EGFR with other members of the HER family results in the limited inhibition. Heterodimer formation is increased in PC-9/ZD cells under basal conditions, and no increase in formation was observed after exposure to gefitinib, although marked heterodimer induction was observed in PC-9 cells. Calculations in *in vitro* studies have shown that the $IC_{50}$-value for inhibition of the tyrosine kinase activity of EGFR is 0.023–0.079 μM, whereas the $IC_{50}$-value for inhibition of HER2 is 100-fold higher.[36] We estimate that the inhibitory effect of gefitinib depends on the ratio of homodimer formation to heterodimer formation, and the heterodimer may be one of the routes of escape from the action of gefitinib.

Signal transduction by the HER family member is mediated by 2 major pathways: the MAPK signaling pathway and the AKT signaling pathway, which regulate cell proliferation and survival. Because phosphorylated AKT was inhibited completely by gefitinib in PC-9 cells, but inhibition of phosphorylated MAPK was not significant, inhibition of the AKT pathway may be more important to cell sensitivity than inhibition of MAPK. Moasser *et al.*[37] reported consistent results, showing that downregulation of AKT activity is predominantly seen in tumors that are sensitive to gefitinib. The phosphorylation of AKT and MAPK was not inhibited significantly by gefitinib in PC-9/ZD cells. This finding might be attributable to inactivation of Tyr 1068-Grb2-SOS-mediated signaling.

Based on the results of this comparative study, EGFR-Grb2-SOS complex formation, phosphorylation of Tyr1068, the ratio of the amount of homodimer formation to heterodimer formation, and the AKT signaling pathway are possible predictive biomarkers for gefitinib sensitivity. As a different approach, we are now looking for the genes associated with gefitinib resistance in PC-9/ZD cells compared to PC-9 cells by subtractive cloning.

## Acknowledgements

'Iressa' is a trademark of the AstraZeneca group of companies.

J_ID: Z3Q Customer A_ID: 04-1248 Cadmus Art: IJC5519 Date: 22-FEBRUARY-05 Stage: I



## References


1. Socinski MA. Addressing the optimal duration of therapy in advanced, metastatic non-small-cell lung cancer. Am Soc Clin Oncol 2003;144–52.
2. Nicholson RI, Gee JM, Harper ME. EGFR and cancer prognosis. Eur J Cancer 2001;37:S9–15.
3. Mendelsohn J, Baselga J. The EGF receptor family as targets for cancer therapy. Oncogene 2000;19:6550–65.
4. Salmon DS, Brandt R, Ciardiello F, Normanno N. Epidermal growth factor-related peptides and their receptors in human malignancies. Crit Rev Oncol Hematol 1995;19:182–232.
5. Fox SB, Smith K, Hollyer J, Greenall M, Hastrich D, Harris AL. The epidermal growth factor receptor as a prognostic marker: result of 370 patients and review of 3009 patients. Breast Cancer Res Treat 1994;29:41–99.
6. Dassonville O, Formento JL, Francoual M, Ramaioli A, Santini J, Schneider M, Demard F. Expression of epidermal growth factor receptor and survival in upper aerodigestive tract cancer. J Clin Oncol 1993;11:1873–8.
7. Sainsbury JR, Farndon JR, Needham GK, Malcolm AJ, Harris AL. Epidermal-growth-factor receptor status as predictor of early recurrence of and death from breast cancer. Lancet 1987;1:1398–402.
8. Scambia G, Benedetti-Panici P, Ferrandina G, Distefano M, Salerno G, Romanini ME, Fagotti A, Mancuso S. Epidermal growth factor, oestrogen and progesterone receptor expression in primary ovarian cancer: correlation with clinical outcome and response to chemotherapy. Br J Cancer 1995;72:361–6.
9. Veale D, Ashcroft T, Marsh C, Gibson GJ, Harris AL. Epidermal growth factor receptors in non-small cell lung cancer. Br J Cancer 1987;55:513–6.
10. Veale D, Kerr N, Gibson GJ, Kelly PJ, Harris AL. The relationship of quantitative epidermal growth factor receptor expression in non-small cell lung cancer to long term survival. Br J Cancer 1993;68:162–5.
11. Druker BJ, Talpaz M, Resta DJ, Peng B, Buchdunger E, Ford JM, Lydon NB, Kantarjian H, Capdeville R, Ohno-Jones S, Sawyers CL. Efficacy and safety of a specific inhibitor of the BCR-ABL tyrosine kinase in chronic myeloid leukemia. N Engl J Med 2001;344:1031–7.
12. Druker BJ, Sawyers CL, Kantarjian H, Resta DJ, Reese SF, Ford JM, Capdeville R, Talpaz M. Activity of a specific inhibitor of the BCR-ABL tyrosine kinase in the blast crisis of chronic myeloid leukemia and acute lymphoblastic leukemia with the Philadelphia chromosome. N Engl J Med 2001;344:1038–42.
13. Joensuu H, Roberts PJ, Sarlomo-Rikala M, Andersson LC, Tervahartiala P, Tuveson D, Silberman S, Capdeville R, Dimitrijevic S, Druker B, Demetri GD. Effect of the tyrosine kinase inhibitor STI571 in a patient with a metastatic gastrointestinal stromal tumor. N Engl J Med 2001;344:1052–6.
14. Fukuoka M, Yano S, Giaccone G, Tamura T, Nakagawa K, Douillard JY, Nishiwaki Y, Vansteenkiste J, Kudoh S, Rischin D, Eek R, Horai T, et al. Multi-institutional randomized phase II trial of gefitinib for previously treated patients with advanced non-small-cell lung cancer. J Clin Oncol 2003;21:2227–9.
15. Kris MG, Natale RB, Herbst RS, Lynch TJ Jr, Prager D, Belani CP, Schiller JH, Kelly K, Spiridonidis H, Sandler A, Albain KS, Cella D, et al. Efficacy of gefitinib, an inhibitor of the epidermal growth factor receptor tyrosine kinase, in symptomatic patients with non-small cell lung cancer: a randomized trial. JAMA 2003;290:2149–58.
16. Giaccone G, Johnson DH, Manegold C, et al. A phase III clinical trial of ZD1839 ('Iressa') in combination with gemcitabine and cisplatin in chemotherapy-naïve patients with advanced non-small-cell lung cancer (INTACT 1). Annual meeting of the European Society for Medical Oncology (ESMO). Nice, France, October 2002.
17. Miller VA, Johnson DH, Krug LM, Pizzo B, Tyson L, Perez W, Krozely P, Sandler A, Carbone D, Heelan RT, Kris MG, Smith R, et al. Pilot trial of the epidermal growth factor receptor tyrosine kinase inhibitor gefitinib plus carboplatin and paclitaxel in patients with stage IIIB or IV non-small-cell lung cancer. J Clin Oncol 2003;21:2094–100.
18. Paez JG, Janne PA, Lee JC, Tracy S, Greulich H, Gabriel S, Herman P, Kaye FJ, Lindeman N, Boggon TJ, Naoki K, Sasaki H, et al. EGFR mutations in lung cancer: correlation with clinical response to gefitinib therapy. Science 2004;304:1497–500.
19. Lynch TJ, Bell DW, Sordella R, Gurubhagavatula S, Okimoto RA, Brannigan BW, Harris PL, Haserlat SM, Supko JG, Haluska FG, Louis DN, Christiani DC, et al. Activating mutations in the epidermal growth factor receptor underlying responsiveness of non-small-cell lung cancer to gefitinib. N Engl J Med 2004;350:2191–3.
20. Pao W, Miller V, Zakowski M, Doherty J, Politi K, Sarkaria I, Singh B, Heelan R, Rusch V, Fulton L, Mardis E, Kupfer D, et al. EGF receptor gene mutations are common in lung cancers from "never smokers" and are associated with sensitivity of tumors to gefitinib and erlotinib. Proc Natl Acad Sci USA 2004;101:13306–11.
21. Nomori H, Saijo N, Fujita J, Hyoi M, Sasaki Y, Shimizu E, Kanzawa F, Inomata M, Hoshi A. Detection of NK activity and antibody-dependent cellular cytotoxicity of lymphocytes by human tumor clonogenic assay—its correlation with the 51Cr-release assay. Int J Cancer 1985;35:449–55.
22. Mosmann T. Rapid colorimetric assay for cellular growth and survival: application to proliferation and cytotoxicity assays. J Immunol Meth 1983;65:55–63.
23. Arteaga CL, Ramsey TT, Shawver LK, Guyer CA. Unliganded epidermal growth factor receptor dimerization induced by direct interaction of quinazolines with ATP binding site. J Biol Chem 1998;273:18623–32.
24. Gorre ME, Mohammed M, Ellwood K, Hsu N, Paquette R, Rao PN, Sawyers CL. Clinical resistance to STI-571 cancer therapy caused by BCR-ABL gene mutation or amplification. Science 2001;293:876–80.
25. Von Bubnoff N. BCR-ABL gene mutation in relation to clinical resistance Lancet 2002;356:487–91.
26. McCormick F. New-age drug meets resistance. Nature 2001;412:281–2.
27. Ricci C, Scappini B, Divoky V, Onida F, Verstovsek S, Kantarjian HM, Beran M. Mutation in the ATP binding pocket of the ABL kinase domain in and STI571-resistant BCR/ABL-positive cell line. Cancer Res 2002;62:5995–8.
28. Laffargue M, Raynal P, Yart A, Peres C, Wetzker R, Roche S, Payrastre B, Chap H. An epidermal growth factor receptor/Gab1 signaling pathway is required for activation of phosphoinositide 3-kinase by lysophosphatidic acid. J Biol Chem 1999;274:32835–41.
29. Rodriguez-Viciana P, Warne PH, Dhand R, Vanhaesebroeck B, Gout I, Fry MJ, Waterfield MD, Downward J. Phosphatidylinositol-3-OH kinase as a direct target of Ras. Nature 1994;370:527–32.
30. Kurata T, Tamura K, Kaneda H, Nogami T, Uejima H, Asai Go G, Nakagawa K, Fukuoka M. Effect of re-treatment with gefitinib ('Iressa', ZD1839) after acquisition of resistance. Ann Oncol 2004;15:173–4.
31. Sugimoto Y. Breast cancer resistance protein (BCRP): physiological substrates, reversing agents and SNPs. Abstract 21. 7th Int Symp Cancer Chemother 2002,Tokyo, Japan, 2002.
32. Naruse I, Ohmori T, Ao Y, Fukumoto H, Kuroki T, Mori M, Saijo N, Nishio K. Antitumor activity of the selective epidermal growth factor receptor- tyrosine kinase inhibitor (EGFR-TKI) Iressatm (ZD1839) in a EGFR-expressing multidrug resistant cell line in vitro and in vivo. Int J Cancer 2002;98:370–5.
33. Reynolds AR, Tischer C, Verveer PJ, Rocks O, Bastiaens PIH. EGFR activation coupled to inhibition of tyrosine phosphatases causes lateral signal propagation. Nat Cell Biol 2003;5:447–53.
34. Haj FG, Markova B, Klaman LD, Bohmer FD, Neel BG. Regulation of receptor tyrosine kinase signaling by protein tyrosine phosphatase-1B. J Biol Chem 2003;278:739–44.
35. Wu JY, Talpaz M, Donato NJ. Tyrosine kinases and phosphatase play a role in STI571-mediate apoptosis of chronic myelogenous leukemia cells. Proc Am Assoc Cancer Res 2003;44.
36. Wakeling AE, Guy SP, Woodburn JR, Ashton SE, Curry BJ, Barker AJ, Gibson KH. ZD1839 (Iressa): an orally active inhibitor of epidermal growth factor signaling with potential for cancer therapy. Cancer Res 2002;62:5749–54.
37. Moasser MM, Basso A, Averbuch SD, Rosen N. The tyrosine kinase inhibitor ZD1839 ("Iressa") inhibits HER2-driven signaling and suppresses the growth of HER2-overexpressing tumor cells. Cancer Res 2001;61:7184–8.

VOLUME 23 · NUMBER 6 · FEBRUARY 20 2005

JOURNAL OF CLINICAL ONCOLOGY

ORIGINAL REPORT

# Randomized Pharmacokinetic and Pharmacodynamic Study of Docetaxel: Dosing Based on Body-Surface Area Compared With Individualized Dosing Based on Cytochrome P450 Activity Estimated Using a Urinary Metabolite of Exogenous Cortisol

*Noboru Yamamoto, Tomohide Tamura, Haruyasu Murakami, Tatsu Shimoyama, Hiroshi Nokihara, Yutaka Ueda, Ikuo Sekine, Hideo Kunitoh, Yuichiro Ohe, Tetsuro Kodama, Mikiko Shimizu, Kazuto Nishio, Naoki Ishizuka, and Nagahiro Saijo*

From the Division of Internal Medicine, National Cancer Center Hospital; Pharmacology Division and Cancer Information and Epidemiology Division, National Cancer Center Research Institute, Tokyo, Japan.

Submitted November 7, 2003; accepted August 19, 2004.

Supported in part by a Grant-in-Aid for Cancer Research (9-25) from the Ministry of Health, Labor, and Welfare, Tokyo, Japan.

Presented in part at the 38th Annual Meeting of the American Society of Clinical Oncology, May 18-21, 2002, Orlando, FL.

Authors' disclosures of potential conflicts of interest are found at the end of this article.

Address reprint requests to Tomohide Tamura, MD, Division of Internal Medicine, National Cancer Center Hospital, 5-1-1, Tsukiji, Chuo-ku, Tokyo, 104-0045, Japan; e-mail: ttamura@ncc.go.jp.



0732-183X/05/2306-1061/$20.00

DOI: 10.1200/JCO.2005.11.036

## ABSTRACT

### Purpose
Docetaxel is metabolized by cytochrome P450 (CYP3A4) enzyme, and the area under the concentration-time curve (AUC) is correlated with neutropenia. We developed a novel method for estimating the interpatient variability of CYP3A4 activity by the urinary metabolite of exogenous cortisol (6-beta-hydroxycortisol [6-β-OHF]). This study was designed to assess whether the application of our method to individualized dosing could decrease pharmacokinetic (PK) and pharmacodynamic (PD) variability compared with body-surface area (BSA) –based dosing.

### Patients and Methods
Fifty-nine patients with advanced non–small-cell lung cancer were randomly assigned to either the BSA-based arm or individualized arm. In the BSA-based arm, 60 mg/m$^2$ of docetaxel was administered. In the individualized arm, individualized doses of docetaxel were calculated from the estimated clearance (estimated clearance = 31.177 + [7.655 × $10^{-4}$ × total 6-β-OHF] − [4.02 × alpha-1 acid glycoprotein] − [0.172 × AST] − [0.125 × age]) and the target AUC of 2.66 mg/L · h.

### Results
In the individualized arm, individualized doses of docetaxel ranged from 37.4 to 76.4 mg/m$^2$ (mean, 58.1 mg/m$^2$). The mean AUC and standard deviation (SD) were 2.71 (range, 2.02 to 3.40 mg/L · h) and 0.40 mg/L · h in the BSA-based arm, and 2.64 (range, 2.15 to 3.07 mg/L · h) and 0.22 mg/L · h in the individualized arm, respectively. The SD of the AUC was significantly smaller in the individualized arm than in the BSA-based arm ($P < .01$). The percentage decrease in absolute neutrophil count (ANC) averaged 87.1% (range, 59.0 to 97.7%; SD, 8.7) in the BSA-based arm, and 87.4% (range, 78.0 to 97.2%; SD, 6.1) in the individualized arm, suggesting that the interpatient variability in percent decrease in ANC was slightly smaller in the individualized arm.

### Conclusion
The individualized dosing method based on the total amount of urinary 6-β-OHF after cortisol administration can decrease PK variability of docetaxel.

*J Clin Oncol 23:1061-1069. © 2005 by American Society of Clinical Oncology*

## INTRODUCTION

Many cytotoxic drugs have narrow therapeutic windows despite having a large interpatient pharmacokinetic (PK) variability. The doses of these cytotoxic drugs are usually calculated on the basis of body-surface area (BSA). Although several physiologic functions are proportional to BSA, systemic exposure to a drug is only partially related to

this parameter.[1-3] Consequently, a large interpatient PK variability is seen when doses are based on BSA. This large interpatient PK variability can result in undertreatment with inappropriate therapeutic effects in some patients, or in overtreatment with unacceptable severe toxicities in others. Understanding interpatient PK variability is important for optimizing anticancer treatments. Factors that affect PK variability include drug absorption, metabolism, and excretion. Among these factors, drug metabolism is regarded as a major factor causing PK variability. Unfortunately, however, no simple and practical method for estimating the interpatient variability of drug metabolism is available. If drug metabolism in each patient could be predicted, individualized dosing could be performed to optimize drug exposure while minimizing unacceptable toxicity.

Docetaxel is a cytotoxic agent that promotes microtubule assembly and inhibits depolymerization to free tubulin, resulting in the blockage of the M phase of the cell cycle.[4] Docetaxel has shown promising activity against several malignancies, including non–small-cell lung cancer, and is metabolized by hepatic CYP3A4 enzyme.[5-15]

Human CYP3A4 is a major cytochrome P450 enzyme that is present abundantly in human liver microsomes and is involved in the metabolism of a large number of drugs, including anticancer drugs.[16-18] This enzyme exhibits a remarkable interpatient variation in activity as high as 20-fold, which accounts for the large interpatient differences in the disposition of drugs that are metabolized by this enzyme.[19-22] Several noninvasive in vivo probes for estimating the interpatient variability of CYP3A4 activity have been reported and include the erythromycin breath test, the urinary dapsone recovery test, measurement of midazolam clearance (CL), and measurement of the ratio of endogenous urinary 6-beta-hydroxycortisol (6-β-OHF) to free-cortisol (FC).[23-27] The erythromycin breath test and the measurement of midazolam CL are the best validated, and both have been shown to predict docetaxel CL in patients.[28,29] However, neither probe has been used in a prospective study to validate the correlations observed, or to test their utility in guiding individualized dosing.

We developed a novel method for estimating the interpatient variability of CYP3A4 activity by urinary metabolite of exogenous cortisol. The total amount of 24-hour urinary 6-β-OHF after cortisol administration (total 6-β-OHF) is significantly correlated with docetaxel CL, which is metabolized by the CYP3A4 enzyme. We also illustrate the possibility that individualized dosing to optimize drug exposure and decrease interpatient PK variability could be performed using this method.[30]

We conducted a prospective, randomized PK and pharmacodynamic (PD) study of docetaxel comparing BSA-based dosing and individualized dosing based on the interpatient variability of CYP3A4 activity, as estimated by a urinary metabolite of exogenous cortisol. The objective of this study was to assess whether the application of our method to individualized dosing could decrease PK and PD variability of docetaxel compared with BSA-based dosing.

## PATIENTS AND METHODS

### Patient Selection

Patients with histologically or cytologically documented advanced or metastatic non–small-cell lung cancer were eligible for this study. Other eligibility criteria included the following: age ≥ 20 years; Eastern Cooperative Oncology Group performance status of 0, 1, or 2; 4 weeks of rest since any previous anticancer therapy; and adequate bone marrow (absolute neutrophil count [ANC] ≥ 2,000/μL and platelet count ≥ 100,000/μL), renal (serum creatinine level ≤ 1.5 mg/dL), and hepatic (serum total bilirubin level ≤ 1.5 mg/dL, AST level ≤ 150 U/L, and ALT level ≤ 150 U/L) function. Written informed consent was obtained from all patients before enrollment onto the study.

The exclusion criteria included the following: pregnancy or lactation; concomitant radiotherapy for primary or metastatic sites; concomitant chemotherapy with any other anticancer agents; treatment with steroids or any other drugs known to induce or inhibit CYP3A4 enzyme[17]; serious pre-existing medical conditions, such as uncontrolled infections, severe heart disease, diabetes, or pleural or pericardial effusions requiring drainage; and a known history of hypersensitivity to polysorbate 80. This study was approved by the institutional review board of the National Cancer Center.

### Pretreatment and Follow-Up Evaluation

On enrollment onto the study, a history and physical examination were performed, and a complete differential blood cell count (including WBC count, ANC, hemoglobin, and platelets), and a clinical chemistry analysis (including serum total protein, albumin [ALB], bilirubin, creatinine, AST, ALT, gamma-glutamyltransferase, alkaline phosphatase [ALP], and alpha-1 acid glycoprotein [AAG]) were performed. Blood cell counts and a chemistry analysis except for AAG were performed at least twice a week throughout the study. Tumor measurements were performed every two cycles, and antitumor response was assessed by WHO standard response criteria. Toxicity was evaluated according to the National Cancer Institute Common Toxicity Criteria (version 2.0).

### Study Design

This study was designed to assess whether the application of our method to individualized dosing could decrease PK and PD variability compared with BSA-based dosing. The primary end point was PK variability and the secondary end point was PD variability (ie, toxicity). In our previous study involving 29 patients who received 60 mg/m$^2$ of docetaxel, the area under the concentration-time curve (AUC) was calculated to be 2.66 ± 0.91 (mean ± standard deviation [SD]) mg/L · h.[30] We assumed that the variability of AUC, represented by the SD, could be reduced by 50% in the individualized arm compared with that in the BSA-based arm, and that AUC would be normally distributed. The required sample size was 25 patients per arm to detect this difference with a two-sided F test at $\alpha = .05$ and a power of 0.914.

Patients were randomly assigned to either the BSA-based arm or individualized arm (Fig 1). In the BSA-based arm, each patient received a dose of 60 mg/m$^2$ of docetaxel. In the individualized arm, individualized doses of docetaxel were calculated from the estimated docetaxel CL after cortisol administration and the target AUC (described in the Docetaxel Administration section).

### Cortisol Administration and Urine Collection

In the individualized arm, 300 mg of hydrocortisone (Banyu Pharmaceuticals Co, Tokyo, Japan) was diluted in 100 mL of 0.9%

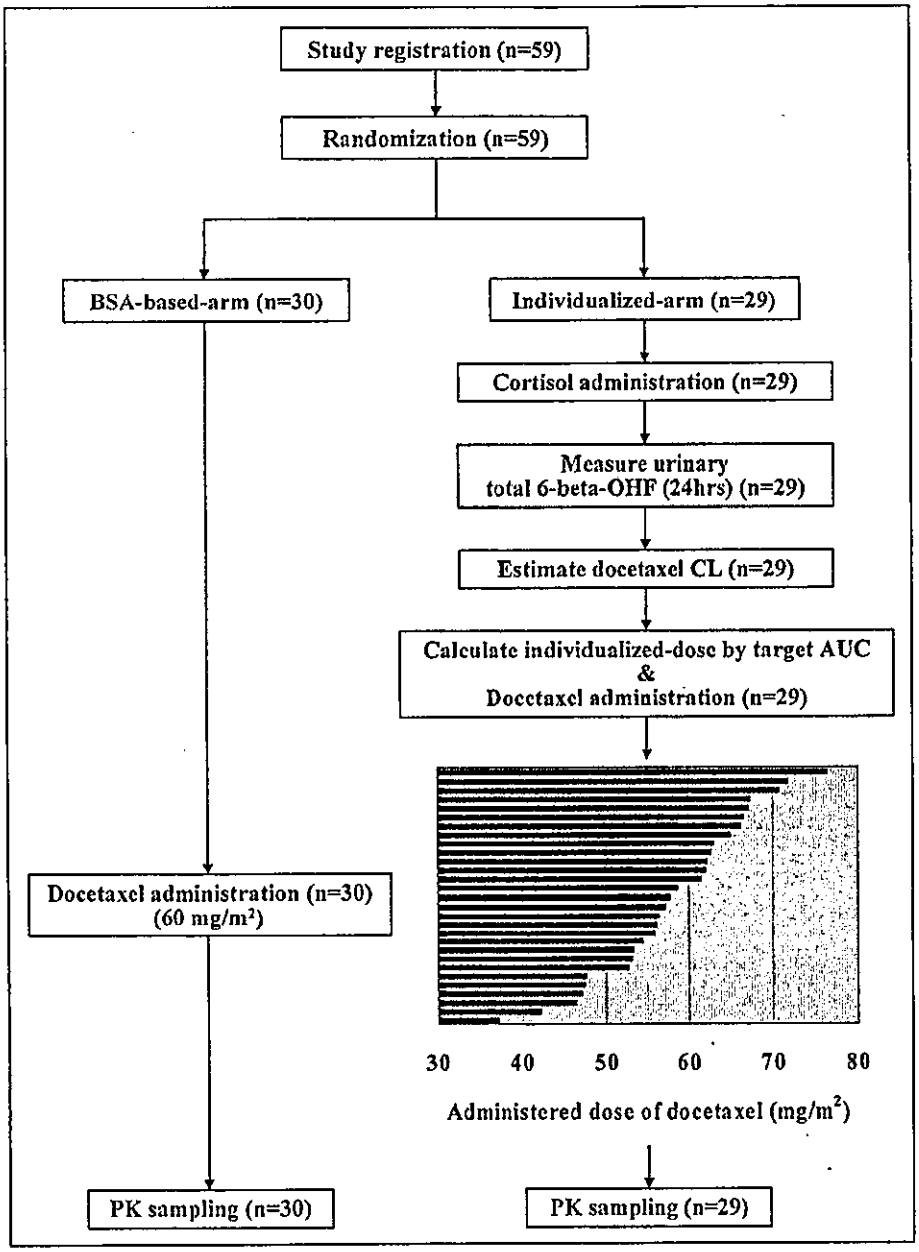


**Fig 1.** Study flow diagram and administered dose of docetaxel. PK, pharmacokinetic; AUC, area under the concentration-time curve; CL, clearance; 6-β-OHF, 6-beta-hydroxycortisol.

saline and administered intravenously for 30 minutes at 9 AM on day 1 in all patients to estimate the interpatient variability of CYP3A4 activity. After cortisol administration, the urine was collected for 24 hours. The total volume of the 24-hour collection was recorded, and a 5-mL aliquot was analyzed immediately.

### *Docetaxel Administration*

Docetaxel (Taxotere; Aventis Pharm Ltd, Tokyo, Japan) was obtained commercially as a concentrated sterile solution containing 80 mg of the drug in 2 mL of polysorbate 80. In the BSA-based arm, a dose of 60 mg/m$^2$ of docetaxel was diluted in 250 mL of 5% glucose or 0.9% saline and administered by 1-hour intravenous infusion at 9 AM to all patients.

In the individualized arm, individualized dose of docetaxel was calculated from the estimated CL and the target AUC of 2.66 mg/L · h using the following equations:

$$\text{Estimated CL (L/h/m}^2) = 31.177 + (7.655 \times 10^{-4} \times \text{total-6-}\beta\text{-OHF [}\mu\text{g/d]}) - (4.02 \times \text{AAG [g/L]}) - (0.172 \times \text{AST [U/L]}) - (0.125 \times \text{age [years]})^{30}$$

$$\text{Individualized dose of docetaxel (mg/m}^2) = \text{estimated docetaxel CL (L/h/m}^2) \times \text{target AUC (2.66 mg/L} \cdot \text{h)}$$

At least 2 days after cortisol administration, individualized doses of docetaxel were diluted in 250 mL of 5% glucose or 0.9% saline and administered by 1-hour intravenous infusion at 9 AM to each patient. The doses of docetaxel in subsequent cycles of treatment were unchanged, and no prophylactic premedication to protect against docetaxel-related hypersensitivity reactions was administered in either of the treatment arms.

### PK Study

Blood samples for PK studies were obtained from all of the patients during the initial treatment cycle. An indwelling cannula was inserted in the arm opposite that used for the drug infusion, and blood samples were collected into heparinized tubes. Blood samples were collected before the infusion; 30 minutes after the start of the infusion; at the end of the infusion; and 15, 30, and 60 minutes and 3, 5, 9, and 24 hours after the end of the infusion. All blood samples were centrifuged immediately at 4,000 rpm for 10 minutes, after which the plasma was removed and the samples were placed in polypropylene tubes, labeled, and stored at −20°C or colder until analysis.

PK parameters were estimated by the nonlinear least squares regression analysis method (WinNonlin, Version 1.5; Bellkey Science Inc, Chiba, Japan) with a weighting factor of 1 per year.[2] Individual plasma concentration-time data were fitted to two- and three-compartment PK models using a zero-order infusion input and first-order elimination. The model was chosen on the basis of Akaike's information criteria.[31] The peak plasma concentration ($C_{max}$) was generated directly from the experimental data. AUC was extrapolated to infinity and determined based on the best-fitted curve; this measurement was then used to calculate the absolute CL (L/h), defined as the ratio of the delivered dosage (in milligrams) and AUC.

To assess PD effect of docetaxel, the percentage decrease in ANC was calculated according to the following formula: % decrease in ANC = (pretreatment ANC − nadir ANC)/(pretreatment ANC) × 100.

### Measurements

The concentration of urinary 6-β-OHF was measured by reversed phase high-performance liquid chromatography with UV absorbance detection according to previously published methods.[30,32,33]

Docetaxel concentrations in plasma were also measured by solid-phase extraction and reversed phase high-performance liquid chromatography with UV detection according to the previously published method.[30,34] The detection limit corresponded to a concentration of 10 ng/mL.

### Statistical Analysis

Fisher's exact test or $\chi^2$ test was used to compare categoric data, and Student's *t* test was used for continuous variables. The strength of the relationship between the estimated docetaxel CL and the observed docetaxel CL was assessed by least squares linear regression analysis. The interpatient variability of AUC for each arm was evaluated by determining the SD and was compared by F test. Biases, or the mean AUC value in each arm minus the target AUC (2.66 mg/L · h), were also compared between the arms by Student's *t* test.

A two-sided *P* value of ≤ .05 or less was considered to indicate statistical significance. All statistical analyses were performed using SAS software version 8.02 (SAS Institute, Cary, NC).

## RESULTS

### Patient Characteristics

Between October 1999 and May 2001, 59 patients were enrolled onto the study and randomly assigned to either the BSA-based arm (n = 30) or the individualized arm (n = 29). All 59 patients were assessable for PK and PD analyses. The pretreatment characteristics of the 59 patients are listed in Table 1. The baseline characteristics were well balanced between the arms except for three laboratory parameters: ALB, AAG, and ALP. These three parameters were not included in the eligibility criteria. The majority of patients (95%) had a performance status of 0 or 1. Twenty (67%) and 16 (55%) patients had been treated with platinum-based chemotherapy in the BSA-based arm and individualized arm, respectively. Only two patients in the individualized arm had liver metastasis, and most of the patients had good hepatic functions.

### Individualized Dosing of Docetaxel

In the individualized arm, the total amount of 24-hour urinary 6-β-OHF after cortisol administration (total 6-β-OHF) was 9,179.6 ± 3,057.7 μg/d (mean ± SD), which was similar to the result of our previous study.[30] The estimated docetaxel CL was 21.9 ± 3.5 L/h/m$^2$ (mean ± SD), and individualized dose of docetaxel ranged from 37.4 to 76.4 mg/m$^2$ (mean, 58.1 mg/m$^2$; Fig 1).

### PK

Docetaxel PK data were obtained from all 59 patients during the first cycle of therapy, and PK parameters are listed in Table 2. Drug levels declined rapidly after infusion and could be determined to a maximum of 25 hours. The concentration of docetaxel in plasma was fitted to a biexponential equation, which was consistent with previous reports.[30,35-38] The mean alpha and beta half-lives were 9.2 minutes and 5.0 hours in the BSA-based arm and 9.2 minutes and 7.4 hours in the individualized arm, respectively.

In the BSA-based arm, docetaxel CL was 22.6 ± 3.4 L/h/m$^2$ (mean ± SD), and AUC averaged 2.71 mg/L · h (range, 2.02 to 3.40 mg/L · h). In the individualized arm, docetaxel CL was 22.1 ± 3.4 L/h/m$^2$, and AUC averaged 2.64 mg/L · h (range, 2.15 to 3.07 mg/L · h). The least squares linear regression analysis showed that the observed docetaxel CL was well estimated in the individualized arm ($r^2$ = 0.821; Fig 2).

The SDs of AUC in the BSA-based arm and in the individualized arm were 0.40 and 0.22, respectively, and the ratio of SD in the individualized arm to that in the BSA-based arm was 0.538 (95% CI, 0.369 to 0.782). The biases from the target AUC in the BSA-based arm and in the individualized arm were 0.047 (95% CI, −0.104 to 0.198) and −0.019 (95% CI, −0.102 to 0.064), respectively, with no significant difference. The interpatient variability of

**Table 1.** Patient Characteristics

| Characteristic | BSA-Based Arm No. of Patients | % | Individualized Arm No. of Patients | % | P |
|---|---|---|---|---|---|
| Enrolled | 30 | | 29 | | |
| Eligible | 30 | 100 | 29 | 100 | |
| Age, years | | | | | .62 |
| Median | 61 | | 62 | | |
| Range | 52-73 | | 45-73 | | |
| Sex | | | | | |
| Male | 25 | 83 | 19 | 66 | .14 |
| Female | 5 | 17 | 10 | 34 | |
| ECOG PS | | | | | |
| 0 | 7 | 23 | 1 | 3 | .08 |
| 1 | 22 | 73 | 26 | 90 | |
| 2 | 1 | 3 | 2 | 7 | |
| Prior treatment | | | | | |
| None | 4 | 13 | 4 | 14 | .99 |
| Surgery | 11 | 37 | 9 | 31 | .65 |
| Radiotherapy | 13 | 43 | 10 | 34 | .49 |
| Chemotherapy | 21 | 70 | 18 | 62 | .52 |
| Platinum-based regimens | 20 | 67 | 16 | 55 | .37 |
| Site of disease | | | | | |
| Lung | 23 | 77 | 28 | 97 | .10 |
| Liver | 0 | 0 | 2 | 7 | .24 |
| Pleura | 8 | 27 | 12 | 41 | .23 |
| Bone | 7 | 23 | 9 | 31 | .71 |
| Extrathoracic lymph nodes | 0 | 33 | 10 | 34 | .93 |
| Laboratory parameters | | | | | |
| ALB, g/L | | | | | .02 |
| Median | 38 | | 35 | | |
| Range | 26-45 | | 24-44 | | |
| AAG, g/L | | | | | .04 |
| Median | 1.00 | | 1.25 | | |
| Range | 0.28-2.15 | | 0.64-2.54 | | |
| AST, U/L | | | | | .67 |
| Median | 21 | | 22 | | |
| Range | 10-40 | | 7-41 | | |
| ALT, U/L | | | | | .88 |
| Median | 18 | | 18 | | |
| Range | 6-54 | | 4-45 | | |
| ALP, U/L | | | | | .03 |
| Median | 249 | | 324 | | |
| Range | 129-540 | | 185-986 | | |

Abbreviations: ECOG, Eastern Cooperative Oncology Group; PS, performance status, ALB, serum albumin; AAG, alpha-1-acid glycoprotein; ALP, serum alkaline phosphatase.

AUC was significantly smaller in the individualized arm than in the BSA-based arm ($P < .01$; Fig 3).

### PD

In both arms, neutropenia was the predominant toxicity related to docetaxel treatment, and 28 of 30 (93%) patients in the BSA-based arm and 25 of 29 (86%) patients in the individualized arm had grade 3 or 4 neutropenia.

**Table 2.** Docetaxel PK Parameters

| Parameters | BSA-Based Arm (n = 30) | Individualized Arm (n = 29) |
|---|---|---|
| $C_{max}$, μg/mL | 0.36-2.70 | 0.99-2.41 |
| $t_{1/2}$ alpha*, minutes | 9.2 ± 3.3 | 9.2 ± 2.7 |
| $t_{1/2}$ beta*, hours | 5.0 ± 4.8 | 7.4 ± 11.7 |
| CL* L/h | 37.6 ± 6.3 | 34.8 ± 7.1 |
| CL* L/h/m² | 22.6 ± 3.4 | 22.1 ± 3.4 |
| AUC | | |
| Mean mg/L · h | 2.71 | 2.64 |
| Range mg/L · h | 2.02-3.40 | 2.15-3.07 |
| Median | 2.65 | 2.66 |
| SD | 0.40 | 0.22 |

Abbreviations: PK, pharmacokinetic; BSA, body-surface area; CL, clearance; AUC, area under concentration-time curve; SD, standard deviation.
*Data represent mean ± SD.

Nonhematologic toxicities, such as gastrointestinal and hepatic toxicities (ie, hyperbilirubinemia, aminotransferase elevations), were mild in both arms.

PD effects shown as the percentage decrease in ANC are listed in Table 3. The percentage decrease in ANC for the BSA-based arm and individualized arm were 87.1% (range, 59.0 to 97.7%; SD, 8.7) and 87.5% (range, 78.0 to 97.2%; SD, 6.1), respectively, suggesting that the interpatient variability in the percentage decrease in ANC was slightly smaller in the individualized arm than in the BSA-based arm (Fig 4). The response rates between the two arms were similar; five of 30 (16.7%) and four of 29 (13.8%) patients

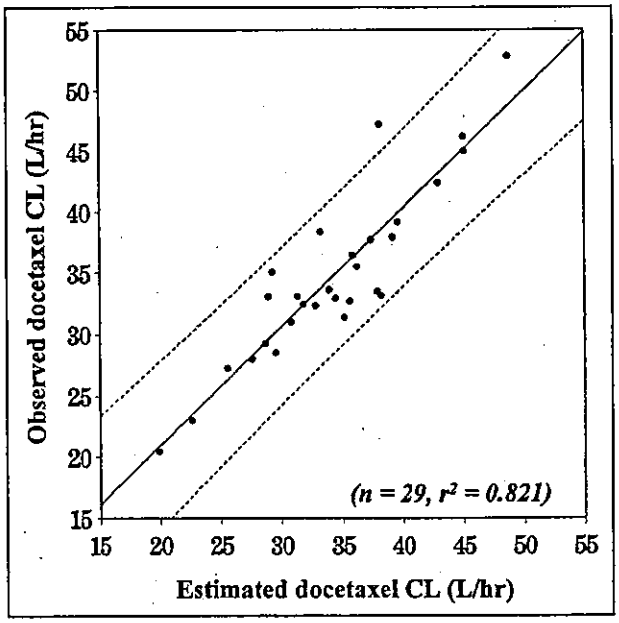


Fig 2. Correlation between the estimated and observed docetaxel clearance (CL) in the individualized arm (n = 29). (—) Linear regression line ($r^2$ = 0.821); (- - - -) 95% CIs for individual estimates.